

56p

N63-13447
code 1

Technical Report No. 32-378

*Resonance Tubes in a
Supersonic Flow Field*

T. Vrebalovich



jpl
JET PROPULSION LABORATORY
CALIFORNIA INSTITUTE OF TECHNOLOGY
PASADENA, CALIFORNIA

July 30, 1962

PRICES SUBJECT TO CHANGE

Reproduced by
**NATIONAL TECHNICAL
INFORMATION SERVICE**
Springfield, Va. 22151

NATIONAL AERONAUTICS AND SPACE ADMINISTRATION
CONTRACT No. NAS 7-100

Technical Report No. 32-378

*Resonance Tubes in a
Supersonic Flow Field*

T. Vrebalovich



John Lauffer, Chief
Gas Dynamics Section

JET PROPULSION LABORATORY
CALIFORNIA INSTITUTE OF TECHNOLOGY
PASADENA, CALIFORNIA

July 30, 1962

Copyright © 1963
Jet Propulsion Laboratory
California Institute of Technology

CONTENTS

I.	Introduction	1
II.	Equipment	3
	A. Wind Tunnel	3
	B. Models	3
	C. Instrumentation of Resonance Tubes	4
III.	Experimental Procedures and Results	6
	A. Round Tube in Thermal Equilibrium	6
	B. Transient Measuring Techniques with the Round Resonance Tube	7
	C. Square Resonance Tube with Glass Sides	9
IV.	Discussion of Results	12
	A. Idealized Resonance Cycle	12
	B. Captured Gas	14
	C. Work at the Contact Surface	15
	D. Estimate of Actual Resonance Cycle	20
	E. Efficiency of Resonance Tube	21
V.	Initiating and Sustaining Features of Resonance Cycle	23
VI.	Conclusions	25
	References	26
	Figures	28

FIGURES

1.	Blunt resonance tube	28
2.	Blunt resonance tube with wing trip and disc gate	29
3.	Blunt resonance tube with ring trip	30

FIGURES (Cont'd)

4.	Glass-sided resonance tube with sharp leading edge and wing trip	31
5.	Effect of plug position on equilibrium temperature distributions in blunt tube	32
6.	Static pressure distribution in blunt tube with wing trip	33
7.	Instantaneous pressure in blunt tube at 5- and 10-in. stations	34
8.	Instantaneous temperature in blunt tube at the plug	35
9.	Effect of ring trip position on equilibrium temperature distribution in blunt tube	36
10.	Effect of trip type, Mach number and water cooling on equilibrium temperature in blunt tube	37
11.	Effect of adding He-A or air on resonant frequency	38
12a.	Spark shadow with disc gate in front of tube	39
12b.	Spark shadow with disc gate removed	39
13.	Oscillograph record of pressures in the tube while the disc gate is being removed	40
14.	Pressures determined from oscillograph record	41
15.	Oscillograph record of thermocouple output while disc gate is being removed	42
16.	Time rate of change of temperature at first instant after disc gate has been removed	43
17.	Pressure at base of glass model without trip	44
18a.	Spark schlieren photograph of glass-sided tube without trip, filling part of cycle	45
18b.	Spark schlieren photograph of glass-sided tube without trip, spilling part of cycle	45
19.	Spark schlieren photograph of glass-sided model with trip	46
20.	Spark schlieren photograph of glass-sided model with trip and knife-edge rotated 180 deg	47
21.	Series of spark schlieren photographs of glass-sided model	48
22.	Pressure at the base, position of shock wave intake, and strength of shock wave in front of the glass-sided tube	49

FIGURES (Cont'd)

23. Idealized resonance cycle	50
24. Work at contact surface in resonance cycle, $P - \bar{x}$ diagram	51

ABSTRACT

13447

Several configurations of resonance tubes were tested in a supersonic wind tunnel to determine the cause of the oscillations and the higher-than-tunnel stagnation temperatures present in the tubes. These tubes were instrumented with pressure transducers, thermocouples, hot wires, and a foreign gas injector. Flow processes in and near the tubes were determined from spark schlieren photographs of a glass-sided model. Heat rates were determined from transient temperature measurements. A cyclic process is proposed, and comparisons between the measured and theoretical predictions are made.

I. INTRODUCTION

Unsteady processes in high-velocity air streams have been arousing increasing interest. The following experimental configurations have been investigated: cutouts in the surface of bodies away from the stagnation region (Ref. 1, 2), cavities in the stagnation region (Ref. 3-5), spikes on blunt-nosed bodies (Ref. 6), and spiked engine diffuser inlets (Ref. 7). A variety of periodic and nonperiodic pressure and shock-wave fluctuations, high heat-transfer rates, and local temperatures higher than the steady-flow recovery temperature have been observed.

In this report, experiments with a resonance tube are described. This tube is a hollow cylinder with one end sealed and the open end placed in a high-velocity jet or in a high-speed wind tunnel parallel to the air flow. Sprenger (Ref. 3) found that such a resonance tube placed in a sonic jet can radiate large-amplitude periodic sound waves and that the base of the tube gets hotter than the stationary free-stream stagnation temperature. He believed that this process might be related to that in the Ranque-Hilsch (Ref. 8, 9) vortex tube in which an air stream is separated into hot and cold parts. Sprenger postulated that a portion of the gas remains in the resonance tube for more than one cycle and is acted on by the intense pressure oscillations in the tube, causing the tube to get hot. He suspected from measurements made with a vibration probe at the base of the tube that shock waves were present in the tube.

Hartmann (Ref. 10) and Dailey (Ref. 11) found large-pressure-amplitude oscillations in certain configurations of resonance tubes, but they did not observe any heating effects. The large mass of these and other experimental configurations precluded the possibility of any temperature increase which could have given a clue to the heat-producing capabilities of resonance tubes. Dailey's experiments were done in conjunction with his investigation of the phenomenon called "diffuser buzz." He used a 1-in. - diameter sharp-lipped total-head tube which could be increased in length up to 60 diameters by moving a plug at the base. He observed large periodic pressure fluctuations at the base with a synchronized motion of the shock wave in front of the tube when the tube was placed in a supersonic air stream. Pressure and flow fluctuations were also observed by Dailey during the buzz cycle of a supersonic spiked inlet diffuser, which subsequently will be compared with the resonance tube.

Recently, Betchov (Ref. 12) analyzed a nonsteady flow similar to that occurring in a resonance tube. This flow was studied experimentally by Lettau (Ref. 13). The tube had one end sealed and an oscillating piston at the other end which could drive the air column in the tube at its characteristic natural frequency.

The column of air developed large-amplitude oscillations in which shock waves were present, and the tube became hot. The pressure wave shape at the stationary base and the flow in the half of the tube nearest the base were similar to the conditions observed in the resonance tube to be described.

The main purpose of the experiments with the resonance tube in supersonic flow was to determine the following:

1. The mechanism and dissipative process for obtaining tube temperatures higher than the tunnel stagnation temperature.
2. The amount of heat that such a process can produce.
3. The reason that the air column in the tube oscillates when the tube is placed in a jet or wind tunnel.

Some of the initial experiments, performed jointly with M. Sibulkin, are discussed in Ref. 4; more recent results are presented in Ref. 14. Results similar to those in Ref. 14 have also been described by Hall and Berry in Ref. 15.

II. EQUIPMENT

A. Wind Tunnel

The experiments were conducted in the Jet Propulsion Laboratory 12-in. supersonic wind tunnel at a Mach number of 2.81. The tunnel could also be evacuated to a pressure of 16 cm Hg in order to calibrate pressure transducers immediately before supersonic flow was established.

B. Models

1. Round, Blunt-Nosed Resonance Tube

The first model consisted of a stainless-steel cylinder with a diameter of 0.722 in. and a wall thickness of 0.016 in., housed in a heavy outer shell to shield the cylinder from the supersonic flow and to protect the attached instrumentation. The positions of the attached thermocouples and the pressure orifices are shown in Fig. 1. The movable plug at the base as well as the pressure transducers on the side of the model are also shown. Bosses were attached at the 2½- and 5-in. positions, and 1/8-in. holes were drilled through the bosses to allow the pressure transducers to be mounted and pressures to be recorded at these stations. The plug, which could be moved as far as 11 in. from the mouth of the tube by an external drive system, could be exchanged easily. This plug was either a microphone, a pressure transducer, a water-cooled diaphragm, a porous plug for injecting or removing gas, or a hot-wire holder. A pair of trombone pipe sections at the rear of the model allowed the plug to be moved while water or gas flowed through the piping connected to the plug. Electrical lead wires were attached on the rear of the model to an extendable helix and were then connected to the instrumentation on the movable plug.

Figure 2 shows the model installed in the tunnel with one of the trips mounted in front of the model. The effect of a trip on resonance will be discussed later. Another trip configuration is shown in Fig. 3. Also shown is a disc gate which could be moved in front of the model to cause the air-column oscillations in the tube to cease. Operated by an air piston with a 2½-in. stroke, the gate could be moved to its extreme positions in a few hundredths of a second. This gate was used in the final phases of the experiment to facilitate accurate pressure measurements before the transducers became hot, and also to make heat-transfer measurements by the transient heat-transfer technique.

2. Square, Glass-Sided Resonance Tube

This resonance tube (Fig. 4) had an inlet 1 in. square and an internal fixed depth of 10.75 in. In contrast to the first configuration, this tube had sharp leading edges and glass sides so that the internal flow could be viewed by both spark schlieren and spark shadowgraph techniques. A pressure transducer, a pressure orifice, and a thermocouple were installed at its base on a piece of 1/8-in. - thick plastic with a 1/8-in.-diameter hole leading to the transducer. The wing trip shown in Fig. 4 could be removed.

C. Instrumentation of Resonance Tubes

Two types of pressure transducers were used to measure static and dynamic pressures in the tubes. One type was a strain-gauge CEC Type 4-312 pressure transducer¹ with a pressure range of 0-60 psia, an over-all diameter of 1/2 in., a diaphragm diameter of 0.45 in., and a frequency response to 8 kc. A standard strain-gauge readout plus a dc amplifier was all that was needed to provide an output for the external instrumentation. This transducer was used at the 2½-in. station of the round resonance tube and at the base of the square tube.

At the 5-in. station and at the plug position in the round tube, the temperatures attained required that water-cooled transducers be used. Water-cooled Photocon Type 363 pressure transducers² with a range of 0-40 psia, a frequency response to 10 kc, an over-all diameter of 0.7 in., a diaphragm diameter of 0.3 in., and a maximum operating temperature of 3000°F were used. Since these transducers had to be interchangeable with the movable plug, they were made smaller in over-all diameter than the standard model. The Photocon Type 363 is a capacitive unit in which the water-cooled diaphragm is one plate of a capacitor. The capacitor is connected to an inductance which is built into the transducer shell to form a tuned circuit. A remote oscillator tuned to 710 kc is link coupled to the inductance in the transducer shell. Changes in capacity due to changes in pressure affect the impedance of the circuit and the output voltage at 710 kc. This 710-kc signal is then demodulated by a diode detector circuit and is fed to an external voltmeter, an oscillograph, and an oscilloscope.

In addition to the transducers which measured static pressures, a series of static-pressure holes in the round tube was connected to either a multimanometer or a pressure switch and a CEC transducer.

¹ Consolidated Electrodynamics Corp., Pasadena, Calif.

² Photocon Research Products, Pasadena, Calif.

A microphone was used in the plug position in the initial phases of the test program to detect the fluctuating pressures in the round tube. A hot wire was mounted 0.012 in. in front and on the center line of the water-cooled diaphragm. A Shapiro-Edwards Model 50B hot wire set³ was used with the hot wire. A Fischer-Porter flowmeter⁴ monitored the flow rate of air or a mixture of 30% helium and 70% argon gas into the porous plug in the model.

Spark schlieren, motion-picture schlieren, and spark shadowgraph pictures were taken of both resonance tubes. For the schlieren photographs the knife edge in the optical system was vertical, and by rotating it 180 deg the shadow properties on the photographs could be reversed.

All of the thermocouples were copper-constantan and were referenced to an ice bath (32°F). These thermocouples were connected to a switch and to a 5-mv Brown indicating potentiometer⁵. A calibrated bucking system could subtract from the thermocouple voltages in 5-mv steps for the measurement of high temperatures.

For transient measurements the thermocouples were connected to an oscillograph, either directly or through dc amplifiers when necessary. The pressure transducers were also connected to the oscillograph. The average static pressure was obtained by filtering the dynamic pressure output with a 1-sec time-constant filter and then feeding this output to the oscillograph via a dc amplifier. The fluctuating pressure was recorded in the same way but was not filtered. The oscillograph film speed was 0.45 in./sec for transient temperature measurements and 115 in./sec for pressure-fluctuation recordings. Pressure fluctuations and the hot-wire output could also be observed on a dual-trace oscilloscope.

³ Shapiro & Edwards, South Pasadena, Calif.

⁴ Fischer & Porter Co., Hatboro, Penn.

⁵ Minneapolis-Honeywell Regulator Co., Philadelphia, Penn.

III. EXPERIMENTAL PROCEDURES AND RESULTS

A. Round Tube in Thermal Equilibrium

When the blunt-nosed round tube without a tripping device was placed in the wind tunnel at $M = 2.81$ and a supply pressure P_0 of 73 cm Hg, no periodic large-amplitude fluctuations or any heating above stagnation conditions were detected, and the pressure at all of the internal pressure taps was pitot pressure P_0' . The addition of a tripping device such as the one shown in Fig. 2 caused the air column in the tube to oscillate at a large pressure amplitude, and the thermocouples near the base indicated temperatures higher than wind-tunnel stagnation temperature. The temperatures attained by the tube were a function of the trip configuration, the trip position, the movable plug position, the stagnation pressure of the wind tunnel, and the Mach number.

Figure 5 shows the temperature distributions obtained after the tube reached thermal equilibrium with the wing trip for several plug positions, where x_p is the distance of the plug from the mouth of the tube. For $x_p = 10$ in. the air column oscillated at 292 cps, which is near the quarter-wavelength closed-end organ-pipe frequency. The static-pressure distribution in the tube obtained from the manometer on the static-pressure orifices is shown in Fig. 6. Moving the plug to different positions did not affect any of the static pressures in front of the plug. In fact, moving the plug to the mouth of the tube had a small effect on the pressures measured on the four orifices outside the tube on the blunt nose.

The pressure fluctuations obtained at the 5-in. and 10-in. stations with $x_p = 10$ in. are shown in Fig. 7. The sharp pressure rise indicates the passage of a shock wave. The absolute-pressure levels could not be determined accurately because of the drift in the transducer calibrations with temperature, so these were determined by the transient technique described in Section III-B.

The instantaneous temperatures were measured with a hot wire 0.0005 in. in diameter, 0.030 in. long, and 0.012 in. from the base of the tube. The high temperatures plus the strong shock waves reflecting from the base of the tube made it difficult to keep even this relatively large-diameter wire in the flow field and to maintain its calibration. Because of the large diameter, and short length of the wire, the wire resistance was so low that it was difficult to determine the instantaneous temperature in the tube accurately; only the temperature wave shape was determined by operating the wire at very low overheat. The wire time constant

was determined approximately and compensated for in the hot-wire amplifier. A comparison of Figs. 7 and 8 shows that the pressure and temperature fluctuations have similar wave shapes, and it is clear that these fluctuations must be in phase.

Equilibrium conditions in the tube were dependent on the tube configuration and tunnel conditions. The effect of moving the trip can be seen in the temperature distributions in Fig. 9, where x_t is the distance of the trip from the mouth of the tube. There is one optimum x_t position for obtaining maximum overheat. The effect of trip shape on overheat is shown in Fig. 10. The ring trip is not as effective as the wing trip. The effect of a subsonic stream on the resonance tube was obtained by operating the supersonic tunnel in an "unstarted" condition, and this result is also plotted in Fig. 10. As can be seen in Fig. 10, water-cooling a thin diaphragm on the plug face reduces the temperatures nearest the plug and removes heat from the gas.

The effect of adding a monatomic gas mixture of 30% helium and 70% argon or air at the porous plug is shown in Fig. 11. Since the speed of sound in helium-argon is higher than in air at the same temperature and density, the resonant frequency of the tube increases as more helium-argon is added, as can be seen in Fig. 11. From the data in Fig. 11 it is clear that adding air at the plug tends to cool the gas and to decrease the resonant frequency.

All of the preceding results were obtained when the tube had reached thermal equilibrium, and they show the effects of tripping devices, helium-argon addition, air addition, heat removal on the resonance-tube cycle, and overheat near the base.

B. Transient Measuring Techniques with the Round Resonance Tube

One of the basic difficulties in making measurements at thermal equilibrium was the zero shift in the pressure transducers resulting from their calibration at room temperature and subsequent operation at temperatures higher than tunnel stagnation temperature near the base of the resonance tube. Therefore, it was necessary to turn the oscillations in the tube on and off and to make measurements only at the onset of resonance before transducer heating could take place. In order to accomplish this, the small disc-gate mechanism described in Section II was constructed. The tunnel was started and reached equilibrium with the disc in front of the tube (see Fig. 2). The gate was opened for several seconds and then closed again. The spark shadow photographs in Figs. 12a and 12b show the gate in both the closed and the open, or resonating, condition.

The transducers were calibrated by first recording the output of the transducers when the model was at atmospheric pressure, and then pumping down the tunnel in several steps to its minimum pressure of 16 cm Hg absolute while these pressures were recorded on the oscillograph. Following this calibration procedure the tunnel was started, and after equilibrium conditions were reached, the oscillograph was operated at its maximum film speed of 115 in./sec for several seconds. The gate was then opened for about 5 sec while the pressures, both average and dynamic, were recorded.

A short piece of the oscillograph record obtained just before and after the gate was opened is shown in Fig. 13 with the base of the tube at the 10-in. position. It takes several cycles before the pressure waves are fully developed. The 2½-in.-station trace shows a sharp pressure step which passes the 5-in. station and is then reflected at the base to arrive back at the 5-in. and at the 2½-in. station. Then the pressure drops first at the 2½-in. station and then at the 5-in. station, and then at the base. It appears that a shock wave propagates down the tube, is reflected from the base, propagates back to the mouth of the tube, and then an expansion wave propagates down the tube. The data in Fig. 14 were determined from this oscillograph trace and are a plot of the minimum and maximum pressures at each transducer, the pressure of the incoming and reflected shock, and the average pressure in the tube at the three transducer stations.

The transient technique was also used to determine at what rate the tube could produce heat. In this case the oscillograph was operated at 0.45 in./sec, and the temperatures were recorded as the gate was removed. A sharp break in the temperature trace of each thermocouple occurs when the gate is removed, as can be seen in Fig. 15, a typical temperature record. At the time when the slope of the temperature traces changes, errors due to conduction along the tube and to the air space surrounding the tube are quite small, since all of the tube and the air space are at the same temperature. As the tube begins to heat, conduction effects become important and the slope of the temperature traces begins to decrease. Therefore, at each thermocouple position the initial temperature-time slope $(dT/dt)_{t \approx 0}$ was measured on the trace and is plotted in Fig. 16. The added mass of the thermocouple leads, the static-pressure lines, the bosses at the transducer stations, and the transducer at the plug position cause the rate of rise of temperature to be different than it would be for a thin cylinder of uniform thickness. The effect of these nonuniformities is approximated by fairing a straight line through the data in Fig. 16. When the tube is assumed to be uniform and the effect of the base is neglected, the heat rate Q is

$$Q = \frac{W C_m}{10''} \int_0^{10''} \frac{dT}{dt} dx$$

where

W = mass of metal in the tube (0.105 lb)

C_m = specific heat of metal (0.12 Btu/lb°F)

When the transducers were not water cooled, the average $dT/dt = 4^\circ\text{F}/\text{sec}$. Therefore $Q = 0.0504$ Btu/sec. In Section IV an estimate of the heat production of an idealized resonating cycle will be compared to this measured value.

C. Square Resonance Tube with Glass Sides

The resonance tube with glass sides and a square cross section was described in Section II-C and shown in Fig. 4. Since this tube had a very large mass and was not insulated, the equilibrium temperature at resonance cannot be compared to that in the round tube. Unlike the round tube, this tube with a sharp-lipped entrance had pressure oscillations of fair amplitude even though no tripping device was used. The pressure wave shape without the wing trip is shown in Fig. 17. This wave has high harmonic content but does not show the sharp rise present in the round tube at resonance. The single spike present in this picture indicates the time that a spark picture was taken. Although shock waves do not seem to be present in the tube, the normal shock wave in front of the tube oscillates back and forth at the same frequency as the pressure at the base of the tube, and spark pictures taken at the extreme positions of this shock are shown in Fig. 18a and b.

The presence of the tripping device shown in Fig. 4 increases the amplitude of oscillation several fold, and shock waves can be seen in the tube. Figures 19 and 20 show typical spark pictures of the flow over the tube and in the tube, where the presence of shock waves is clearly indicated by the dark and light vertical lines in the tube. These pictures were also synchronized with the pressure at the base. With the trip the pressure wave shape at the base is similar to that in the round tube and also indicates the presence of shock waves in the tube. Since these schlieren pictures were taken with a vertical knife edge, the direction of propagation of shock waves within the tube can be determined by noting whether the shock waves are dark or light and comparing them with the shock wave in front of the tube. It is then clear in Fig. 19 that a dark shock within the tube indicates a high pressure upstream and a low pressure downstream, showing that the shock is propagating down the tube, and vice versa for a light shock in the tube. The spark photograph in Fig. 20 was obtained by rotating the knife edge in the schlieren system 180 deg, which makes

the incoming shock clearer than that in Fig. 19. These spark pictures also show the effects of inflow and outflow on the external shock system.

The spark schlieren pictures of the glass-sided model were synchronized with the pressure at the base of the tube. The oscilloscope was operated in the single sweep position where the first increase in input voltage from the pressure transducer triggered the sweep after the "reset" button was pushed. The main sweep sawtooth voltage on the oscilloscope was biased such that by changing the bias a thyatron could be triggered at any given time during the sweep. The thyatron fired the spark for the schlieren picture. A small portion of the thyatron output was superimposed on the signal from the pressure transducer to indicate, by a sharp spike in the signal, exactly when the spark was fired.

With this technique it was possible to make a composite of a number of spark photographs to determine the position of the internal shock at any given time. A typical set of spark pictures is shown in Fig. 21. Frames 1 and 2 show the shock propagating down the tube and reflecting back to the mouth of the tube. The flow near the mouth of the tube becomes supersonic in Frame 2 since oblique shock reflections appear near the mouth. In Frame 3 the reflected shock seems to blend into these shocks and is barely detectable at the 2 1/2-in. position. In fact, the shock system in Frame 3 looks similar to the "shock train" found in diffusers near Mach 1.

An $x-t$ diagram of the internal shock position and pressure at the base of the tube is shown in Fig. 22. The circled numbers on the pressure trace refer to the time that the schlieren pictures in Fig. 21 were taken. The shock waves are not very strong, and from the data of Fig. 22 the shock speed seems to be fairly constant for both the shock wave propagating down the tube and that reflecting back to the mouth.

The external flow field in the previous schlieren pictures looks similar to that of a choked supersonic spike diffuser in the presence of buzz. When the shock wave reflects from the base and arrives at the mouth, the shock in front steepens rapidly and the flow in the tube spills because the shock wave arriving at the mouth reflects an expansion wave. While the tube spills, the internal flow is void of shock waves. The flow over the wing trip during this cycle is of interest since it seems to be a key to the sustaining feature of the oscillation. In Frame 1 of the cycle in Fig. 21 the flow over the trip is separated and becomes almost fully attached in Frame 2 while the tube is still in the compression cycle. When the shock wave reflects from the base and passes over the wing, the flow over the wing separates, the shock in front steepens, and the flow over the wing remains separated while the air in the tube spills. Then the separated region narrows and disappears in the compression part of the cycle. By measuring the angle of

the oblique shock wave attached to the wing trip, the shock strength vs time can be determined and compared to the pressure at the base and to the position of the shock wave in the tube. Figure 22a is such a plot. At the expected time that the reflected shock should be expelled from the tube the shock strength of the oblique shock on the wing trip increases rapidly, remains strong while the tube spills, and then slowly diminishes in strength until the tube is filled again. The synchronized spark-schlieren technique with the glass-sided resonance tube therefore gives a clear picture of the time history of the resonance cycle.

IV. DISCUSSION OF RESULTS

If air is brought to rest in a steady adiabatic wind-tunnel flow field, the maximum temperature that the air can attain is the supply-section stagnation temperature. In the case of oscillating flow in the resonance tube there are two features in the unsteady flow that cause the temperatures in the tube to exceed the tunnel stagnation temperature. It will be shown that the tube gets hot because (1) a certain amount of the air within the tube remains for more than one resonance cycle and (2) shock waves propagate through this air and are the main dissipative process.

A. Idealized Resonance Cycle

From both the synchronized spark-schlieren photographs of the square tube and the pressure and temperature wave shapes that were recorded, it has been shown that when the flow in the tube is resonating there are shock waves in the resonance tube during a part of each cycle. From the instantaneous pressure measurements in the round tube, an idealized resonance cycle may be constructed. Part of the idealized resonance cycle that is chosen is similar to the shock tube cycle. A sketch of the $x-t$ diagram of an equilibrium cycle with the pressures labeled is shown in Fig. 23a, and the position of the shock waves, contact surface, and expansion waves in the tube for different parts of the cycle are shown in Fig. 23b. The main boundary condition on the cycle is the repetition of the pressure cycle. That is, after the passage of the incoming shock, reflected shock, and the expansion waves the tube returns to the initial minimum pressure and the cycle repeats.

The idealized cycle can be simply described from the sketch in Fig. 23b. Let the cycle start with uniform temperature and pressure in the tube, T_1 and P_1 (Fig. 23b-1). There is a contact surface at the mouth of the tube that separates the gas in the tube from that in the surrounding tunnel. A shock wave propagates down the tube with a pressure P_2 behind the shock, and the contact surface moves down the tube with the velocity that would exist behind this normal shock wave (Fig. 23b-2). The shock wave reflects from the base, and as it moves toward the mouth of the tube it brings to rest at pressure P_3 all gas through which it passes (Fig. 23b-3). Shock reflections that might arise when the shock wave passes through the contact surface are neglected. When the shock wave passes the mouth of the tube it reflects an expansion wave which empties the tube back to the initial minimum pressure isentropically. If at some time during the equilibrium cycle enough heat Q is removed to cause the gas to return to the initial temperature T_1 , then $T'_1 = T_1$.

If the initial pressure is P_1 and the pressure behind the incoming shock is P_2 , the temperature ratio across the shock, T_2/T_1 , may be determined from P_2/P_1 by using the normal shock relations.

The pressure ratio due to the reflected shock at the base of the tube is

$$\frac{P_3}{P_2} = \frac{\left(2 \frac{\gamma-1}{\gamma+1} + 1\right) \frac{P_2}{P_1} - \frac{\gamma-1}{\gamma+1}}{\frac{\gamma-1}{\gamma+1} \frac{P_2}{P_1} + 1} \quad (1)$$

where P_3 is the pressure behind the reflected shock wave. If the tube is insulated and no heat is removed during the cycle, the isentropic expansion from P_3 to P_1 does not return the gas to T_1 but to T_1' . From the isentropic relation

$$\frac{T_1'}{T_3} = \left(\frac{P_1}{P_3}\right)^{\gamma-1/\gamma} \quad (2)$$

$$T_1' = T_1 \frac{T_3}{T_2} \frac{T_2}{T_1} \left(\frac{P_1}{P_2} \frac{P_2}{P_3}\right)^{\gamma-1/\gamma}$$

It can be shown that $T_1' \geq T_1$, and the gas is then hotter at the end of the cycle than at the beginning. In fact, no matter what the starting point of the cycle, it can be shown that $T_2' \geq T_2$, $T_3' \geq T_3$, etc.

The temperature rise per cycle for the insulated case can then be calculated from the measurements plotted in Fig. 14. The minimum pressure measured was 6 cm Hg at the 5- and 10-in. positions and about 8 cm Hg at the 2 1/2-in. position where the plug was at the 10-in. position. The pressure level behind the incoming shock at the 2 1/2- and 5-in. positions was 16 cm Hg, and the measured level of the reflected shock was 37 cm Hg. From the shock relations, if $P_1 = 6$ cm Hg and $P_2 = 16$ cm Hg, then $P_2/P_1 = 2.665$ and $T_2/T_1 = 1.360$. Substituting P_2/P_1 in Eq. (1), gives $P_3/P_2 = 2.345$. Therefore $P_3 = 37.5$ cm Hg, which is equal to the measured reflected shock pressure within the accuracy of the measurements. From the shock

relations for the reflected shock, $T_3/T_2 = 1.298$. Substituting for the determined pressure and temperature ratios in Eq. (2) results in $T'_1 = 1.046 T_1$. It can also be shown that $T'_2 = 1.046 T_2$ and $T'_3 = 1.046 T_3$.

Since each cycle raises the temperature level of the captured gas about 5%, if most of the hot gas at minimum pressure were to remain within the tube from cycle to cycle, at the 292-cps rate a compound interest formula leads to a temperature so high that real-gas effects would appear in the insulated case. Of course, conduction effects and spillage provide a practical limitation on this temperature.

B. Captured Gas

This idealized cycle, and the results of the helium - argon addition experiment, now make it possible to estimate the amount of gas that remains in the tube for more than one cycle. A gas mixture of 30% helium and 70% argon with a ratio of specific heats of 1.67 and a density near that of air was added through a porous plug at the base of the tube. Since the speed of sound in this mixture of helium - argon is higher than that of air at the same temperature and density, the resonant frequency of tube should increase as more He - A is added. That is, the compression and expansion waves should move faster through a gas containing some He - A than through air and thereby increase the resonant frequency of the tube. The results (Fig. 11) show that the resonant frequency increases, then levels off and decreases because of the cooling effect of the gas, as can also be seen from the effect of cold-air addition on the resonant frequency.

In the resonance cycle the captured gas is that gas which is still in the tube at the end of the expansion part of the cycle. At this time in the cycle the gas in the tube is at its lowest pressure and temperature. A uniform pressure of 6 cm Hg and a temperature of 360°F are assumed to exist in the tube in Fig. 11. The captured gas is then that gas which started behind the contact surface at this lowest pressure and remains behind the contact surface and in the tube.

The only way that captured gas may escape after an equilibrium cycle is reached is by the mixing that takes place near the contact surface. If a tangent is drawn as shown in Fig. 11, the intercept is then a fair approximation of the spillage, which is then about 10% of the captured gas. The spillage may be defined as that portion of the captured gas which has been heated by the dissipative processes (shock waves and skin friction) in the tube during a cycle which, owing to mixing and diffusion at the contact surface, is spilled into the external flow field outside the tube at the end of a cycle. At most, even if the maximum in the curve were used, only 20% would be spilled. If all of the gas in the tube were helium and argon, the resonant frequency would be 318 cps as compared to 292 cps for air at the same temperature. Even if the

temperature of the added helium - argon gas were the same as that of the air, a frequency of 318 cps could not be attained since the shock waves and expansion waves always pass through air during part of the cycle. Therefore, 10% spillage is probably an overestimate, and at least 90% or more of the initial captured gas is retained in the tube for the next cycle.

C. Work at the Contact Surface

Another way of considering the heat-producing ability of a resonant cycle is to determine the work that is done on the captured gas by the external gas. Since the contact surface is the only moving boundary on the captured gas, the work done at the contact surface is that done by the external flow field on the captured gas. Since the flow conditions are known at the contact surface, the work done by the contact surface may be calculated and a cycle drawn in the $P-x$ plane. Consider that all of the heat is removed at P_3 in a constant pressure process such that the expansion to P_1 is isentropic. Then the cycle in the $P-\bar{x}$ diagram is that shown in the sketch in Fig. 24, where \bar{x} is the distance of the contact surface from the base of the tube (i.e., $\bar{x} = 10 - x$). On the $P-\bar{x}$ diagram it should be noted that from the previous notation on the $t-x$ diagram (Fig. 22), $T_a = T_1$, $T_b = T_c = T_2$, and $T_d = T_3$. At $\bar{x} = x_a, x_c, x_d$, and x_e the specific volume is proportional to \bar{x} , and \bar{x} is used instead of the specific volume in the gas law and isentropic relations. From the $P-x$ diagram it can also be seen that $x_a = x_b$ and $x_c = x_d$.

The work done on the captured gas by the contact surface in the cycle is $W = - \oint F d\bar{x} = -A \oint P d\bar{x}$, where A is the area of the tube. Therefore,

$$W = -A \left\{ \int_a^b P d\bar{x} + \int_b^c P d\bar{x} + \int_c^d P d\bar{x} + \int_d^e P d\bar{x} + \int_e^a P d\bar{x} \right\} \quad (3)$$

$$W_{a-b} = W_{c-d} = -A \int_{x_a}^{x_b} P dx = -A \int_{x_c}^{x_d} P dx = 0 \quad (4)$$

since $x_a = x_b$ and $x_c = x_d$. The contact surface moves at constant pressure P_2 until the reflected shock intersects the surface. The work done by the contact surface in the compression part of the cycle is

$$W_{b-c} = -A \int_{x_b}^{x_c} P d\bar{x}$$

From the perfect-gas law

$$\frac{x_d}{x_a} = \frac{P_1}{P_3} \frac{T_d}{T_a}$$

$$x_d = x_c = \frac{P_1}{P_2} \frac{P_2}{P_3} \frac{T_d}{T_b} \frac{T_b}{T_a} x_a$$

and all of these pressure and temperature ratios are either measured or determined from the normal shock relations. Therefore,

$$W_{b-c} = -AP_2 \int_{x_b}^{x_c} d\bar{x} = -AP_2 (x_c - x_b)$$

$$W_{b-c} = -AP_1 x_a \left(\frac{P_2}{P_1} - \frac{P_2}{P_3} \frac{T_d}{T_b} \frac{T_b}{T_a} \right) \quad (5)$$

Next, consider the isentropic expansion from e to a , where enough heat Q has been removed at P_3 so that W_{e-a} is an isentropic expansion.

$$W_{e-a} = -A \int_{x_e}^{x_a} P d\bar{x}$$

and the isentropic relations are

$$P\bar{x}^\gamma = P_1 x_a^\gamma = P_3 x_e^\gamma$$

$$\frac{T_e}{T_a} = \left(\frac{P_3}{P_1} \right)^{\gamma-1/\gamma}$$

Then

$$\bar{x} = \frac{P_1^{1/\gamma} x_a}{P}$$

$$\frac{d\bar{x}}{dx} = - \frac{\bar{x} dP}{\gamma P}$$

Substituting the isentropic relations into W_{e-a} , gives

$$W_{e-a} = \frac{-AP_1^{1/\gamma} x_a}{\gamma} \int_{P_1}^{P_3} P^{-1/\gamma} dP$$

$$W_{e-a} = \frac{-AP_1 x_a}{\gamma-1} \left[\left(\frac{P_3}{P_1} \right)^{\gamma-1/\gamma} - 1 \right]$$

or

$$W_{e-a} = \frac{-AP_1 x_a}{\gamma-1} \left[\frac{T_e}{T_a} - 1 \right] \tag{6}$$

In order to calculate W_{d-e} , the isentropic relations are needed again to determine T_e . The perfect-gas law gives

$$\frac{x_d}{x_e} = \frac{T_d}{T_e}$$

and substituting for x_d results in

$$x_e = \frac{T_e}{T_a} \frac{P_1}{P_2} \frac{P_2}{P_3} x_a$$

The work is

$$W_{d-e} = -A \int_{x_d}^{x_e} P dx$$

$$W_{d-e} = -AP_3 (x_e - x_d)$$

Therefore,

$$W_{d-e} = -AP_1 x_a \left(\frac{T_e}{T_a} - \frac{T_d}{T_b} \frac{T_b}{T_a} \right) \quad (7)$$

The total work per cycle is then the sum of Eq. (4), (5), (6), and (7):

$$W = W_{a-b} + W_{b-c} + W_{c-d} + W_{d-e} + W_{e-a}$$

$$W = -AP_1 x_a \left[\left(\frac{P_2}{P_1} \frac{P_2}{P_3} \frac{T_d}{T_b} \frac{T_b}{T_a} \right) + \left(\frac{T_e}{T_a} \frac{T_d}{T_b} \frac{T_b}{T_a} \right) + \frac{1}{\gamma-1} \left(\frac{T_e}{T_a} - 1 \right) \right] \quad (8)$$

The work done in this cycle is then simply determined from the given initial minimum pressure, the pressure behind the incoming shock wave, the shock relations, the perfect-gas law, the isentropic relations, and the physical dimensions of the tube. The pressures needed were measured and presented in Section IV-A. From the shock relations,

$$\frac{P_2}{P_1} = 2.665; \quad \frac{T_b}{T_a} = \frac{T_2}{T_1} = 1.360$$

From the reflected shock strength,

$$\frac{P_3}{P_2} = 2.345; \quad \frac{T_d}{T_b} = \frac{T_3}{T_2} = 1.298$$

From the isentropic relation,

$$\frac{T_e}{T_a} = \frac{T_e}{T_1} = \frac{P_3}{P_1}^{\gamma-1/\gamma} = 1.687$$

Substituting in Eq. (8) gives $W = 0.271 AP_1 x_a$.

But

$$A = \frac{\pi D^2}{4} = 2.84 \times 10^{-3} \text{ ft}^2$$

$$P_1 = 6 \text{ cm Hg} = 166.5 \text{ lb/ft}^2$$

$$x_a = 10 \text{ in.}$$

Therefore the work per cycle is

$$W = 1.370 \times 10^{-4} \text{ Btu}$$

Since the frequency is 292 cps, the work per second \bar{W} is

$$\bar{W} = 292 W$$

$$\bar{W} = 0.0400 \text{ Btu/sec}$$

Since the heat is removed at the maximum pressure P_3 such that the cycle repeats, the amount of heat removed $Q = \bar{W}$. The measured $Q = 0.0504$ Btu/sec compares favorably with the Q determined by the idealized resonance cycle.

D. Estimate of Actual Resonance Cycle

The experimental observations show several obvious shortcomings to the idealized cycle which has been described. There are two details which have been overlooked which would increase the estimated heat rate. The first is that the pressure of the captured gas at the base of the tube continues to increase to $P_4 = 52$ cm Hg after the reflected shock passes through it. In the $P-x$ diagram of Fig. 24, the dotted portion of the cycle takes into account the fact that the pressure is increasing while the heat is being removed. The possible amount of work available if all of the heat were removed during this portion of the cycle would be 0.044 Btu/sec, which is about 88% of the measured value. The second, the effect of the skin friction, is considered to be small compared to the shock-wave effects and cannot easily be estimated from the available measurements.

Those factors which result in an overestimate of the heating capacity of the resonance tube will now be considered. The spillage rate of less than 10% of the captured gas causes an overestimate in the available heat rate by less than 10%. Even though the captured gas is at its maximum temperature and pressure for about half the cycle, during which time heat is conducted from it, it is clear that heat is also conducted to the walls at other than this maximum condition; and, of course, heat is conducted to the gas from the walls during that part of the cycle when the gas is cooler than the walls. This would tend to reduce the cyclic heating rate. Since the incoming shock does not originate at the mouth of the tube and does not immediately reach full strength, there is then an overestimate of the work done by the contact surface during the compression part of the cycle.

A detailed construction of an $x-t$ diagram by the method of characteristics is also possible. The pressure-time history is known at several stations in the resonance tube, and these could be used as part of the boundary condition. An iterative procedure would have to be employed to determine the boundary condition on the flow field at the mouth of the tube. Unfortunately, even a detailed $x-t$ diagram would involve some assumptions concerning the amount of heat removed from the captured gas during various further parts of the cycle.

Some perspective into what further information an $x-t$ diagram might reveal can be gained by inspecting Rudinger's (Ref. 16) example of a gas at high pressure in a tube expanding into a low-pressure region. He found that the expansion waves propagate to the base, reflect as expansion waves at the base, propagate to the mouth, and reflect as weak pressure waves which coalesce near the mouth of the tube to form shock waves. The shock wave propagates to the base, reflects to the mouth, and the cycle repeats with a decaying amplitude. Incidentally, the synchronized spark pictures of the square tube never indicated the presence of a shock wave nearer than $2\frac{1}{2}$ -in. from the mouth of the tube, which checks with Rudinger's $x-t$ construction. Several features which have been neglected in the idealized cycle become evident in Rudinger's example. The tube is not at uniform pressure when the incoming and reflected shocks propagate through the gas, and the contact surface continues to move toward the base after the passage of the reflected shock, as has already been surmised.

The primary purpose of the experiment was not to make a detailed comparison of the potential and actual heating rates, but to determine the flow phenomena responsible for this heating above stagnation tunnel temperatures. The fact that the measured and estimated heating rates are in close agreement is indeed fortunate and indicates that the idealized cycle adequately describes the phenomena.

E. Efficiency of Resonance Tube

The efficiency of the resonance tube can be determined by comparing the heat rate with the increase in drag due to oscillation. As has been noted already, moving the plug in the round tube from the 10-in. position to the mouth of the tube had no effect on the static pressures measured in front of the plug and on the nose of the tube. Therefore, the increase in drag ΔD is identically equal to the difference in force on the plug face when it is at the base and when it is at the mouth of the tube. From the measurements in Fig. 6,

$$P_{base\ average} = P_b = 31\text{ cm Hg}$$

$$P_{mouth\ average} = P_m = 19\text{ cm Hg}$$

$$A = \text{area of tube opening} = 2.84 \times 10^3\text{ ft}^2$$

$$\Delta D = A(P_b - P_m)$$

$$\Delta D = 0.944\text{ lb}$$

The drag work is then

$$W_{D/sec} = U\Delta D, \text{ where } U = 1970 \text{ ft/sec}$$

$$W_{D/sec} = 2.39 \text{ Btu/sec}$$

The efficiency is

$$\eta = \frac{Q}{W_{D/sec}}$$

$$\eta = 2.1\%$$

where $Q = 0.0504 \text{ Btu/sec}$.

The resonance tube is not an efficient heater. The effect of resonance on the external flow field during a cycle, the fact that the reflected shock propagates through a large mass of gas which is spilled, plus the spillage of the captured gas, all contribute to the drag and not to the heating of the tube.

V. INITIATING AND SUSTAINING FEATURES OF RESONANCE CYCLE

The experimental results and the simplified theory of the resonance cycle explain why the resonance tube gets hot, but the mechanism that initiates and sustains the resonance cycle is not clear. A key to the understanding of this mechanism may lie in the configurations which do or do not excite oscillations. There were no large-amplitude oscillations in the blunt-nosed resonance tube without a trip; whereas oscillations were present in the sharp-lipped, square resonance tube without a trip. The main difference between the flow fields over these two configurations was that there was a separated region at the sharp lip of the square tube outside of the tube. It is well known that separated regions exist at the convex corner of blunt cylindrical models in supersonic flow, and it is to be expected that the sharp-lipped tube would have a separated region even if there were no oscillations in the tube. As can be seen in Fig. 18a and 21 (frames 5, 6, and 7) there is a separated region originating at the sharp lip, and the size of the region changes during the resonance cycle.

In the sharp-lipped resonance tube and before the onset of oscillation, the stagnation stream line has a stagnation point inside the tube near the lip, but definitely not at the sharp corner of the lip. Any disturbance in the flow field could cause the stagnation point to move and change the size of the separated region. A change in the angle of attack of a wing on which there is leading edge separation has an effect on the stagnation point and size of the separated region similar to that of a disturbance for the sharp-lipped tube. Since the separated region affects the shock shape and flow field in front of the tube, and since any change in the flow field can change the stagnation line, we can surmise that there is a feedback mechanism which might be the source for initiating and sustaining the oscillations in the tube. Any pressure disturbance propagating to the base of the tube is reflected back to the mouth of the tube to further upset the stagnation line position, and the length of the tube determines the resonant frequency of the cyclic oscillations. Therefore, it seems that the lip of the square resonance tube could act as a source of edge tones in the same manner as does a sharp lip in acoustic problems (Ref. 10) and, in fact, during a resonant cycle, a ring vortex is shed by the tube.

The effect of the tripping device is to change the boundary conditions near the mouth of the tube and act as a source of edge tones for the blunt-nosed body. The separated region over the wing trip during part of the cycle (Fig. 21) is caused by the interaction of the reflected shock wave from the tube with the trip boundary layer. The shock strength on the wing can vary between a weak oblique shock to an almost

normal strong shock. This shock condition in front of the tube, and the fact that the pressure of the shock wave reflected from the fixed base in the tube is higher than that of the normal shock wave arriving at the base, are important in determining the amplitude of the pressure fluctuations in the tube.

VI. CONCLUSIONS

It was found that certain configurations of resonance tubes in supersonic and high-speed subsonic wind tunnel flow fields exhibited large amplitude pressure oscillations with accompanying temperatures in the tubes higher than the free-stream stagnation temperature. From spark schlieren photographs of a glass-sided tube and from pressure and temperature wave shapes in these tubes, it was determined that shock waves were present in the tubes. By injecting a mixture of helium and argon at the base of the tube, it was found that there is a captured gas that remains within the tube for more than one cycle. The heating rate of the resonant cycle was also measured.

A cyclic model was proposed which included a shock tube process for part of the cycle. This approximate cycle, which considered the work done on the captured gas together with the measured instantaneous pressures in the tube, gave an estimate for the heating rate of the cycle which was nearly equal to the measured value. A possible mechanism for initiating and sustaining resonance is also proposed.

Although the external flow field of resonance tube configurations may differ for different experiments, it is clear that the basic reason for resonance tube heating is the presence of the shock wave in the tube, which is the main dissipative process in these tubes. Unfortunately, it is not possible to determine *a priori* whether a given tube configuration will exhibit resonance, nor is it possible to predict the amplitude of the oscillations, the maximum temperatures, or the heating rate of any particular configuration. It is well to note that certain configurations such as those with sharp lips or trips or tubes near jets should be avoided where the resonance effects might be destructive.

ACKNOWLEDGMENT

The author wishes to thank M. Sibulkin, who proposed the problem and initiated the work described herein, P. Wegener, J. Laufer, and C. Thiele, who made helpful suggestions, J. Edberg, who aided in the wind tunnel testing, W. Simms, who designed the electronics, A. Kistler and R. Betchov, who contributed to many rewarding discussions, and (Mrs.) Diana Menkes, who edited much of the material incorporated in the present paper.

REFERENCES

1. Chapman, D. C., Kuehn, D. M., and Larson, H. K., *Investigation of Separated Flows in Supersonic and Subsonic Streams with Emphasis on the Effect of Transitions*, NACA Technical Note No. 3869, March 1957.
2. Krishnamurty, K., *Acoustic Radiation from Two-Dimensional Rectangular Cutouts in Aerodynamic Surfaces*, NACA Technical Note No. 3487, August 1955.
3. Sprenger, H. S., "Über Thermische Effekte bei Resonanzrohren," *Mitteilungen aus dem Institut für Aerodynamik an der E.T.H.*, Zurich, Nr. 21, pp. 18-35, 1954. (A.E.R.E. Lib/Trans. 687.)
4. Sibulkin, M. and Vrebalovich, T., "Some Experiments with a Resonance Tube in a Supersonic Wind Tunnel," *J. Aero. Sci.*, Vol. 25, No. 7, p. 465, July 1958.
5. Johnson, R. H., *An Instability in the Hypersonic Flow about Blunt Bodies*, General Electric Research Laboratories, Report No. 58-RL-2074, September 1958.
6. Stalder, J. R. and Nielsen, H. V., *Heat Transfer from a Hemisphere-Cylinder Equipped with Flow-Separation Spikes*, NACA Technical Note No. 3287, September 1954.
7. Dailey, C. L., "Supersonic Diffuser Instability," *J. Aero. Sci.*, Vol. 22, No. 11, pp. 733-749, November 1955.
8. Ranque, G., "Expériences sur la détente giratoire avec productions simultanées d'un échappement d'air chaud et d'un échappement d'air froid," *J. Phys. Radium*, (7) 4, pp. 112-114, 1933.
9. Hilsch, R., "Die Expansion von Gasen im zentrifugalfeld als Kälteprozess," *Z. Naturforsch.*, 1, pp. 208-212, 1946.
10. Hartmann, J., "On the Production of Acoustic Waves by Means of an Airjet of a Velocity Exceeding that of Sound," *Phil. Mag.*, 7, Vol. 11, No. 72, pp. 926-948, April 1931.
11. Dailey, C. L., *Investigation of Supersonic Diffuser Instability*, USCEC Report 41-3, March 1955.
12. Betchov, R., "Nonlinear Oscillations of a Column of Gas," *Phys. Fluids*, Vol. 1, No. 3, pp. 205-212, May-June 1958.

REFERENCES (Cont'd)

13. Lettau, E., "Messungen an Gasschwingungen grober Amplitude in Rohrleitungen," *Deutsch Kraftfahrtforschung im Auftrag des Reichs-Verkehrsministeriums*, Heft 39, 1939.
14. Vrebalovich, T., "Resonance Tube in Supersonic Flow," 10th Anniversary Meeting of Division of Fluid Dynamics, Am. Phys. Soc., Bethlehem, Pennsylvania, November 1957 (*Bull. Am. Phys. Soc.* 3, p. 291, 1958).
15. Hall, I. M. and Berry, C. J., "On the Heating Effect in a Resonance Tube," Readers' Forum, *J. Aero. Sci.*, Vol. 26, No. 4, p. 253, April 1959.
16. Rudinger, G., *Wave Diagrams for Nonsteady Flow in Ducts*, Van Nostrand, New York, 1955.

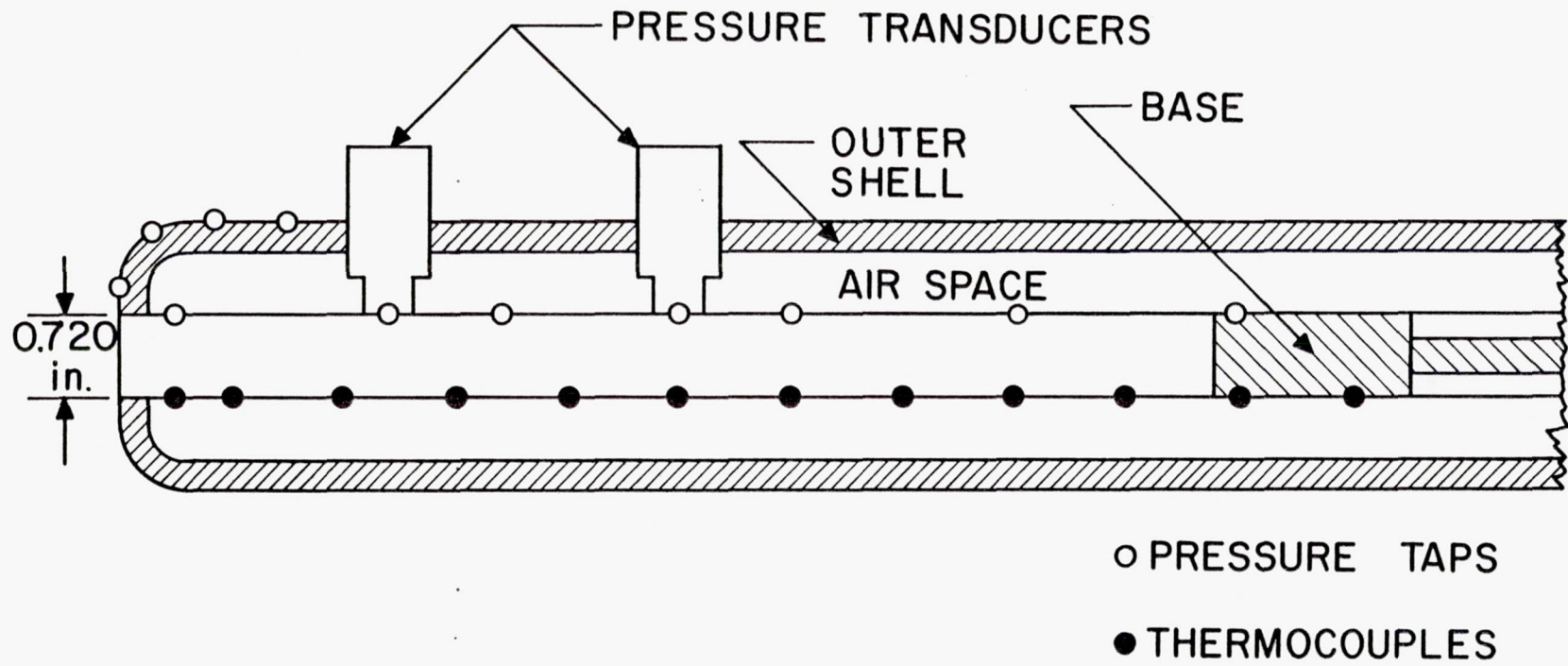


Fig. 1. Blunt resonance tube

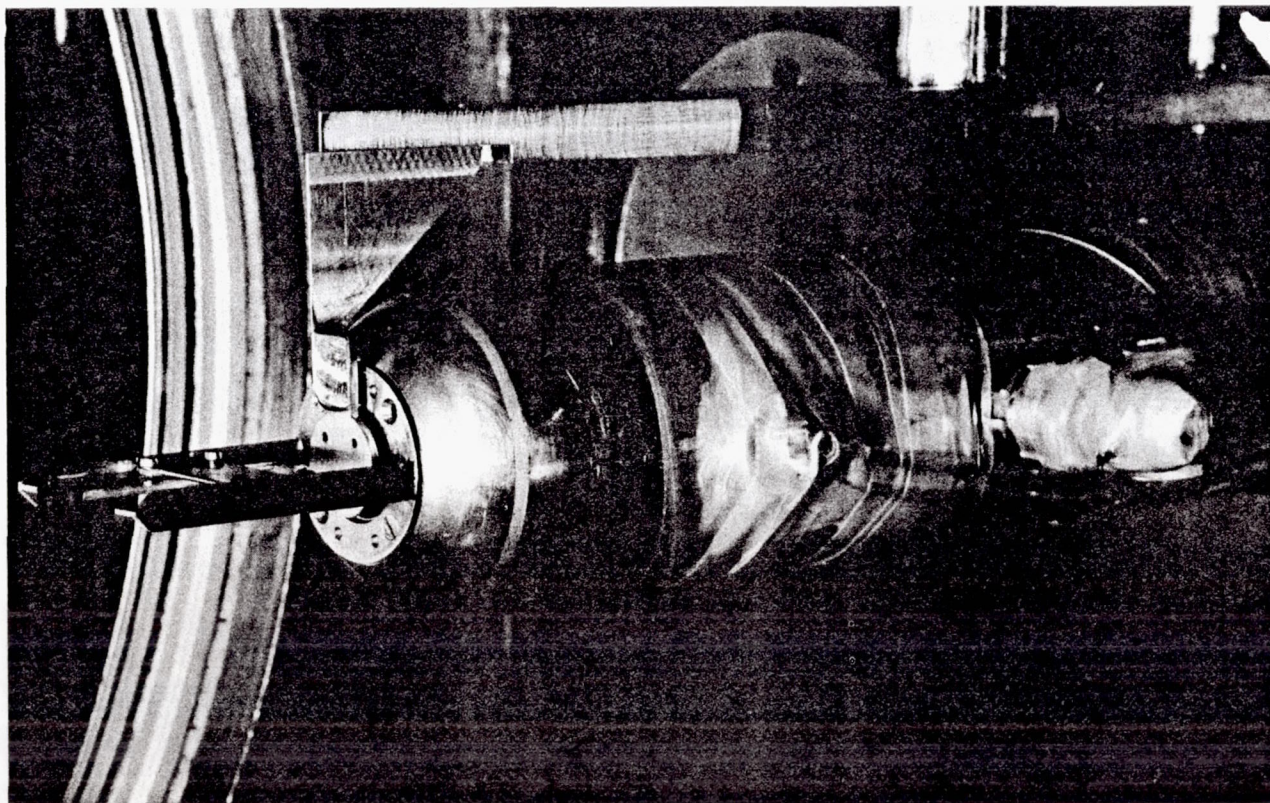


Fig. 2. Blunt resonance tube with wing trip and disc gate

NOT REPRODUCIBLE

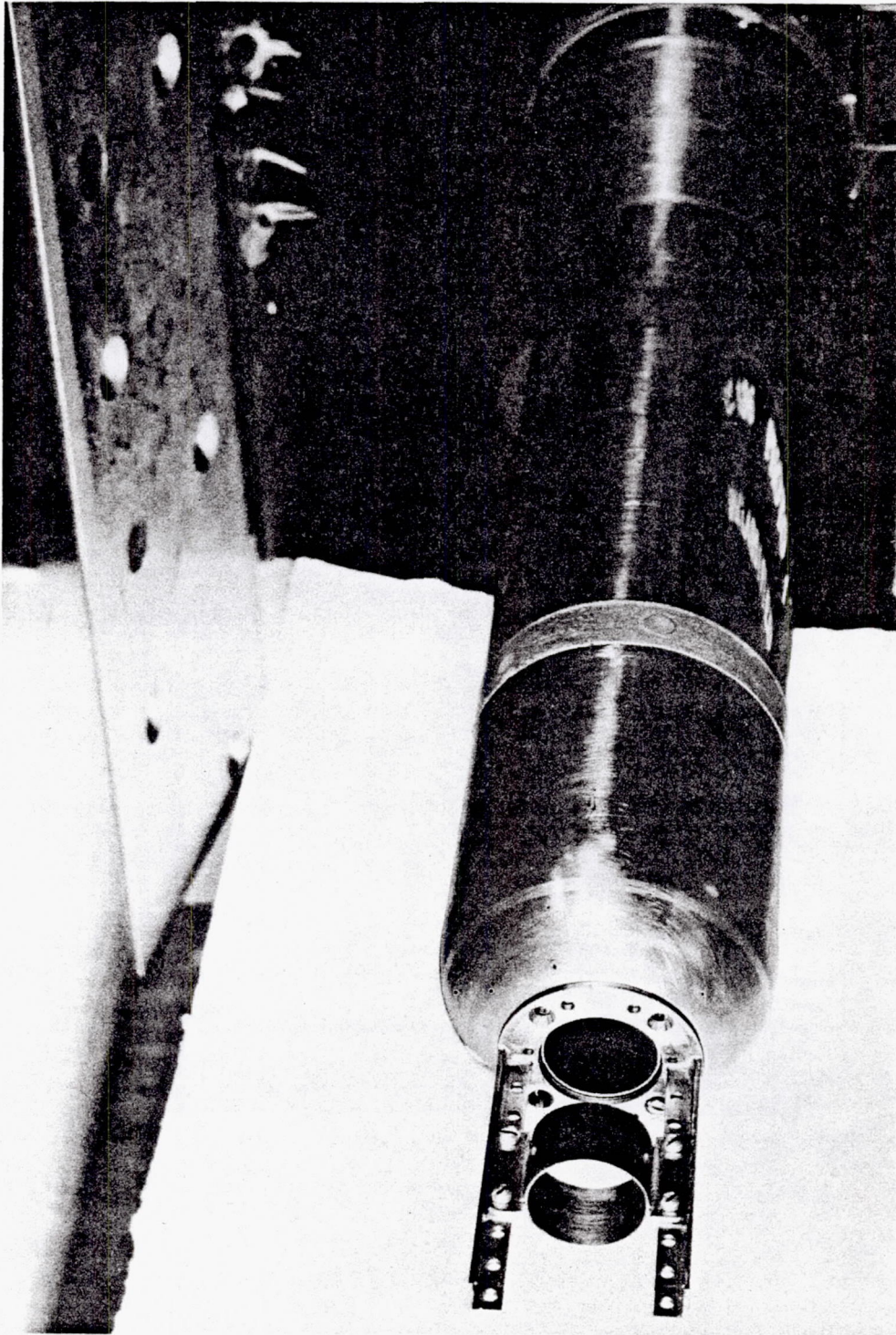


Fig. 3. Blunt resonance tube with ring trip

NOT REPRODUCIBLE

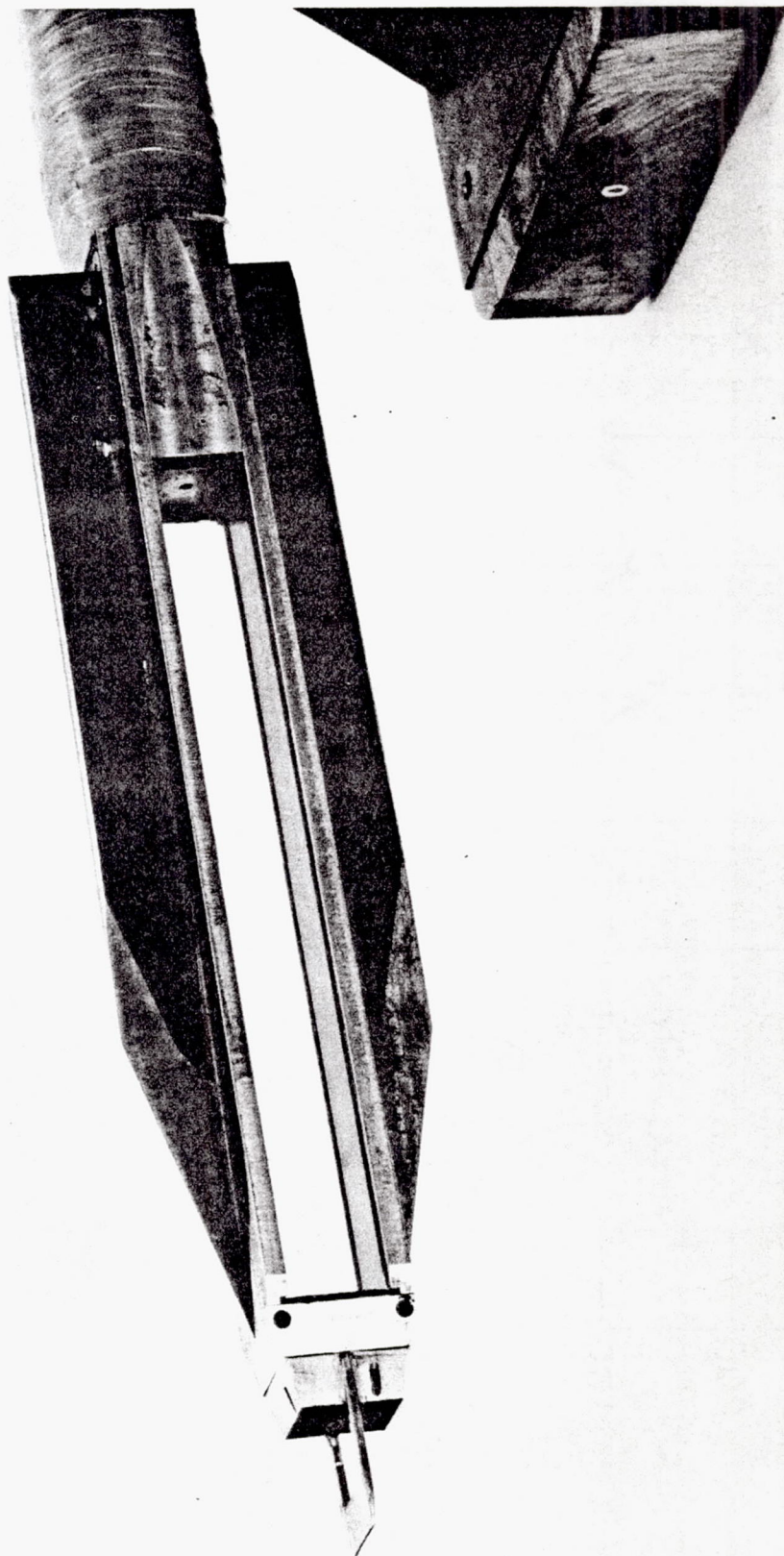


Fig. 4. Glass-sided resonance tube with sharp leading edge and wing trip

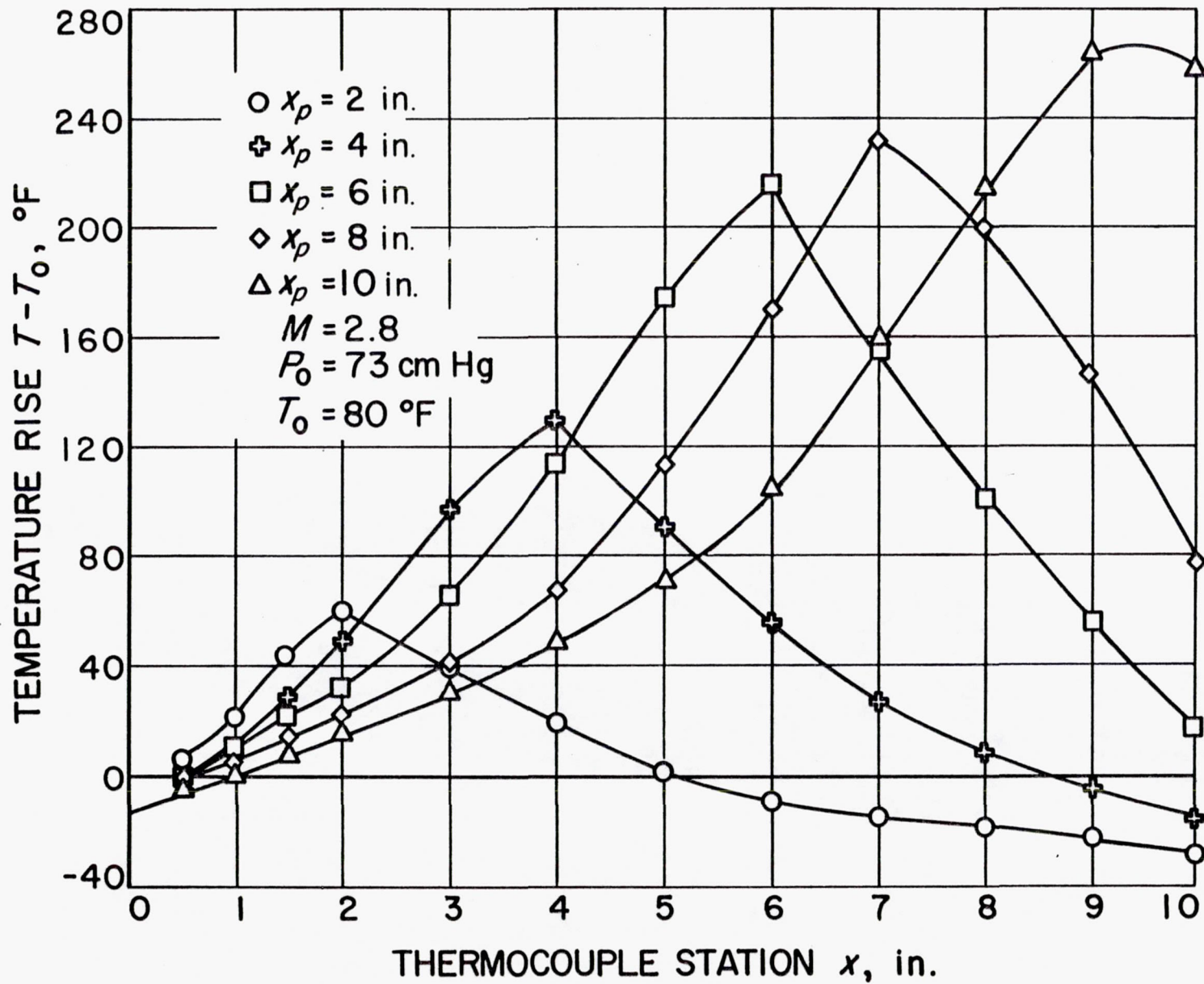


Fig. 5. Effect of plug position on equilibrium temperature distributions in blunt tube with wing trip

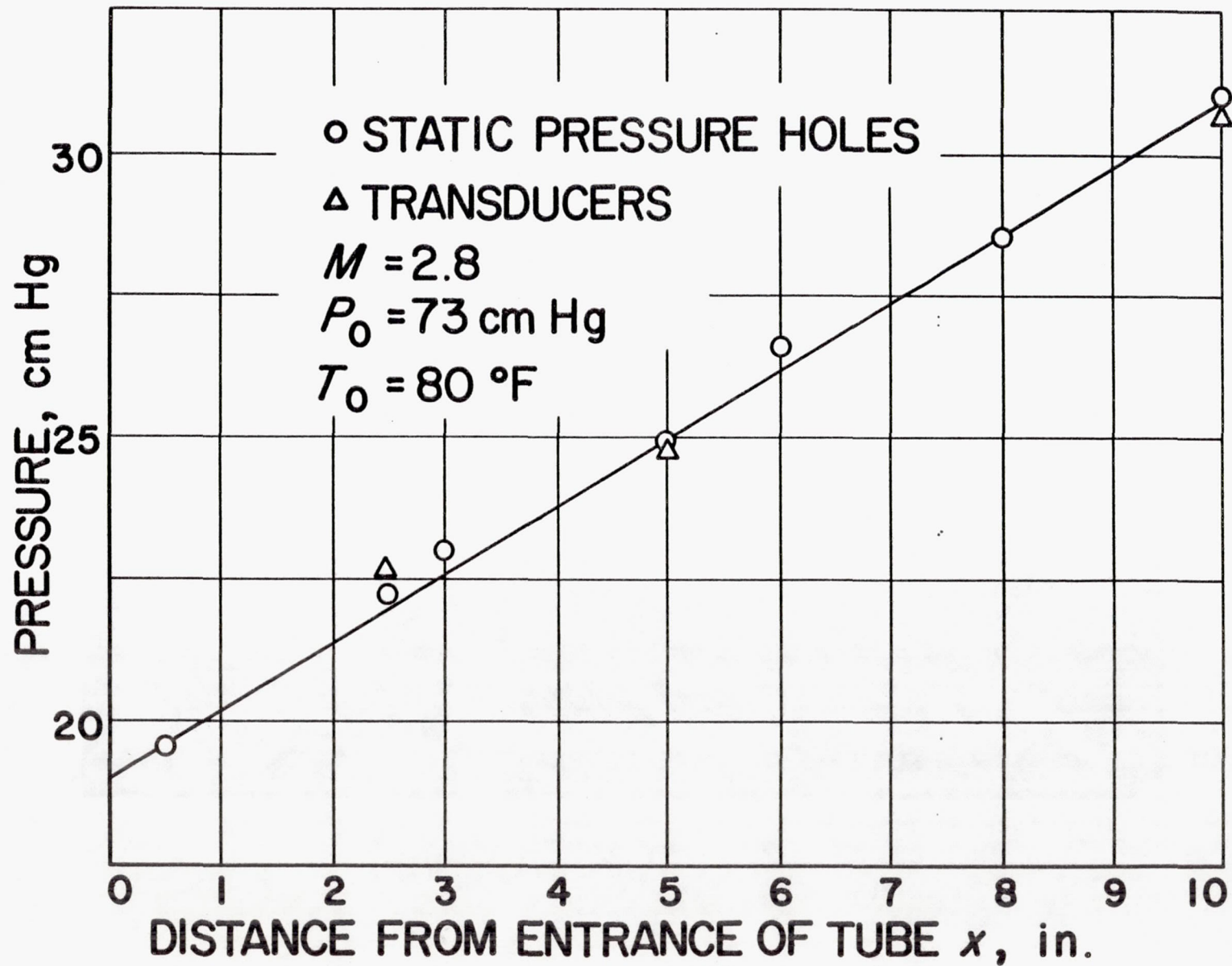


Fig. 6. Static pressure distribution in blunt tube with wing trip

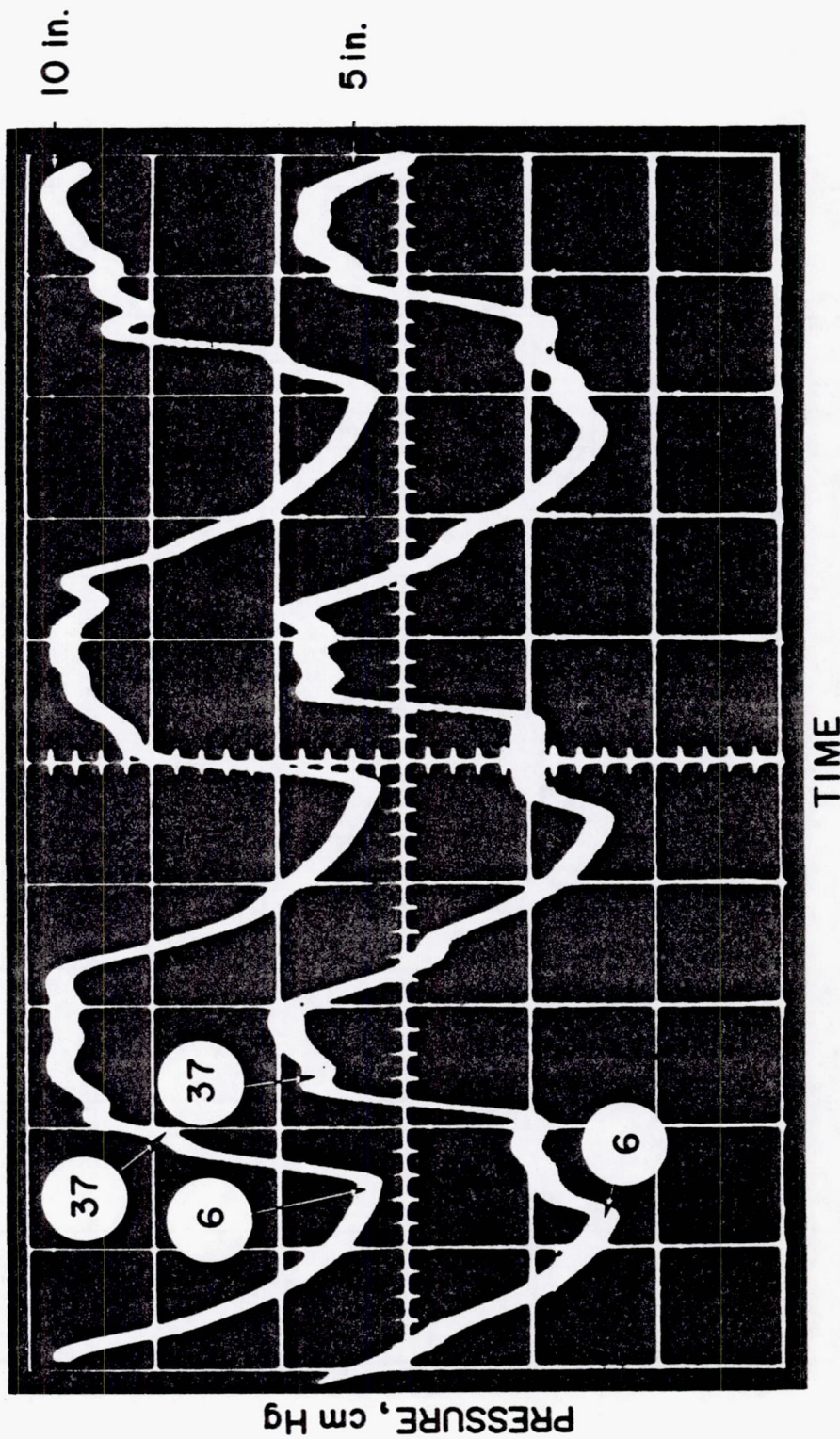


Fig. 7. Instantaneous pressure in blunt tube at 5- and 10-in. stations

NOT REPRODUCIBLE

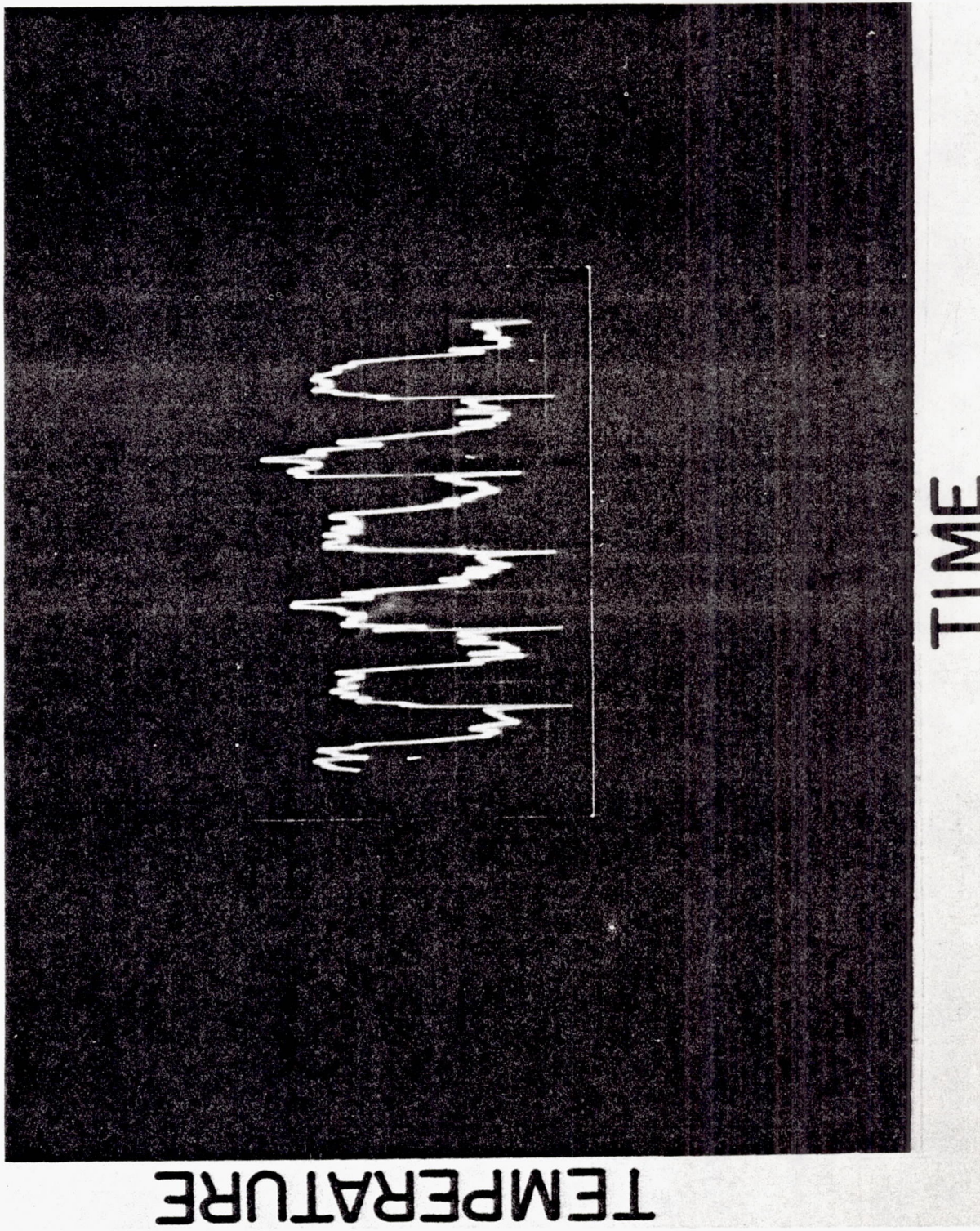


Fig. 8. Instantaneous temperature in blunt tube at the plug

NOT REPRODUCIBLE

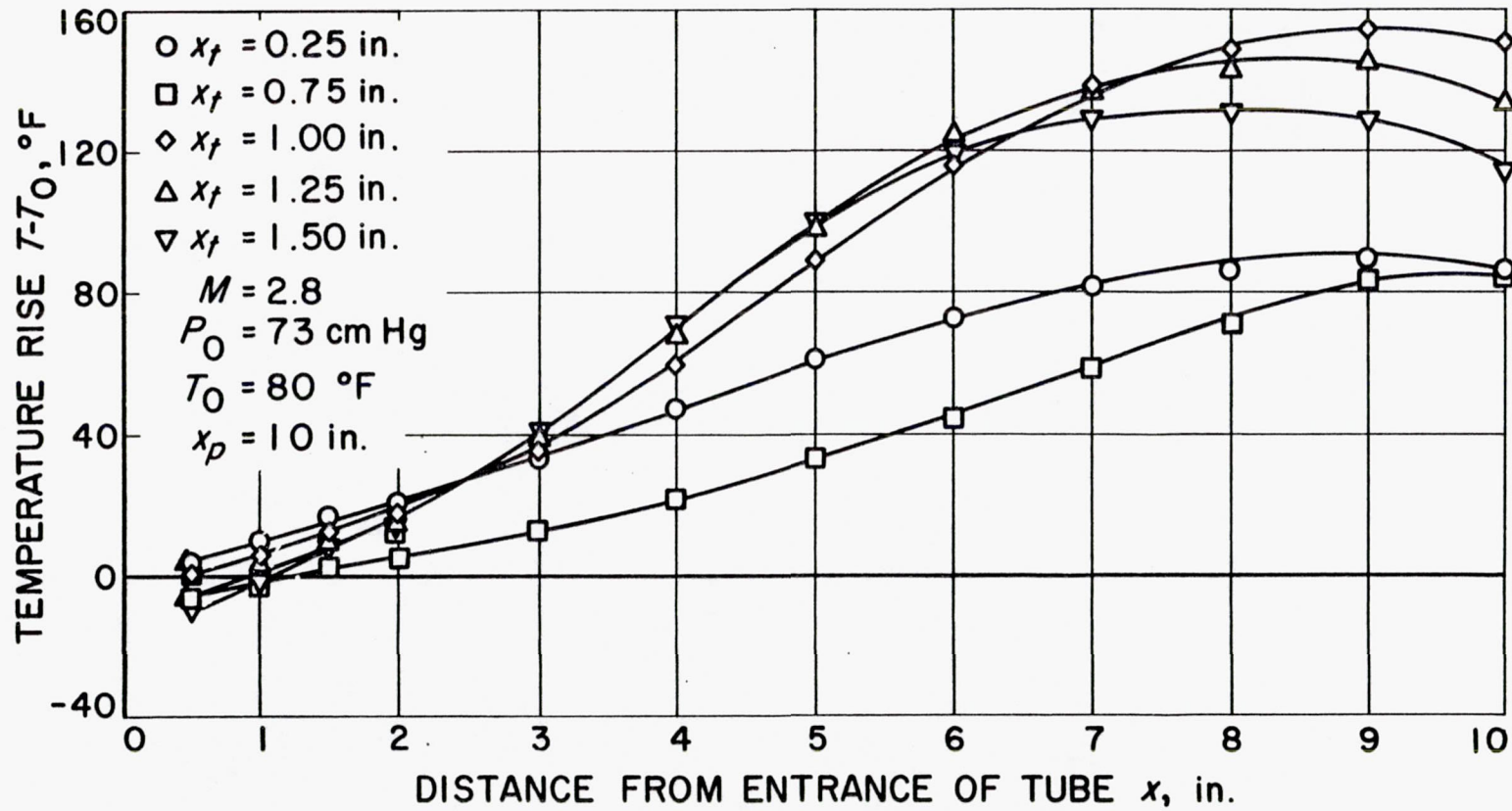


Fig. 9. Effect of ring trip position on equilibrium temperature distribution in blunt tube

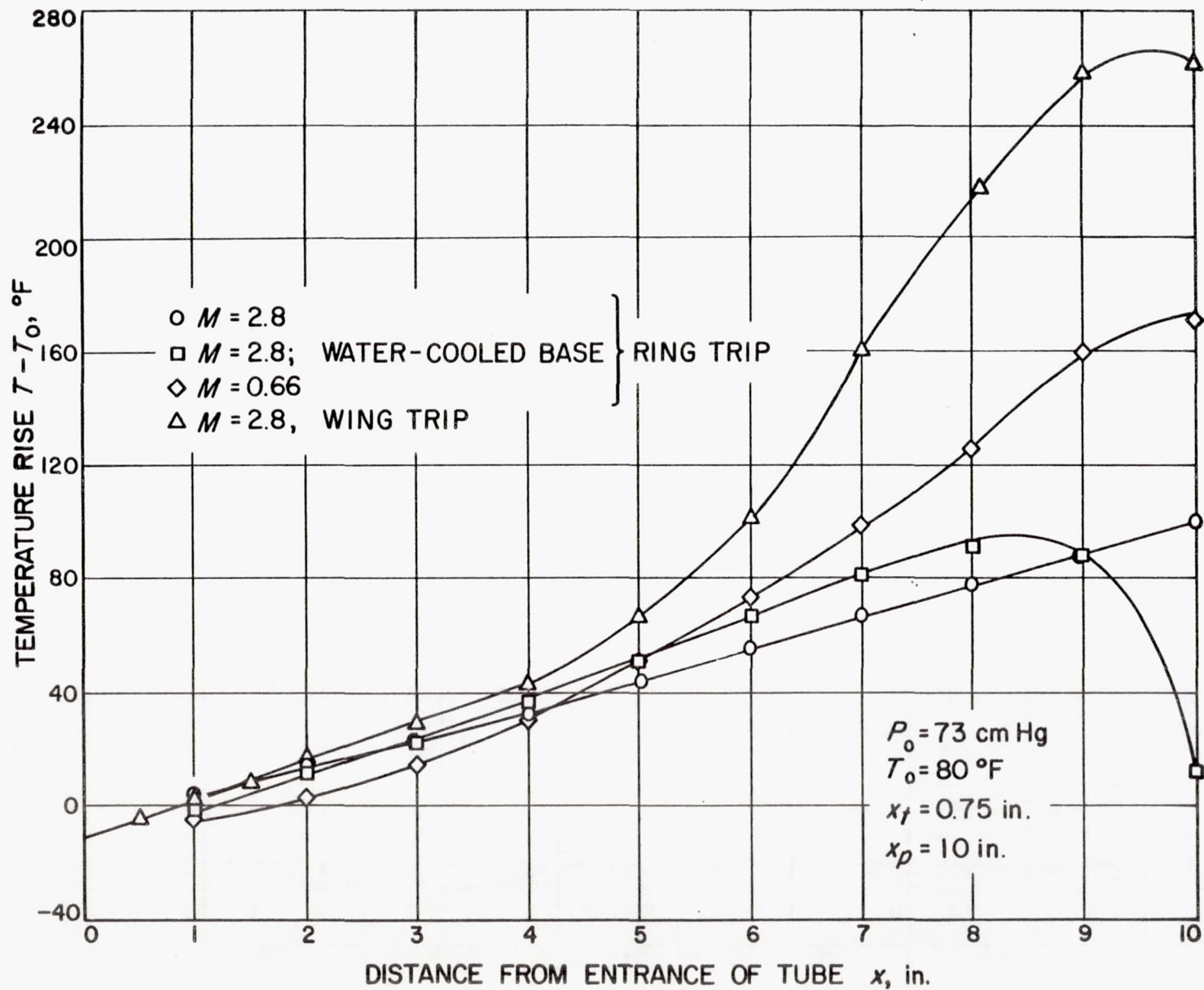


Fig. 10. Effect of trip type, Mach number and water cooling on equilibrium temperature in blunt tube

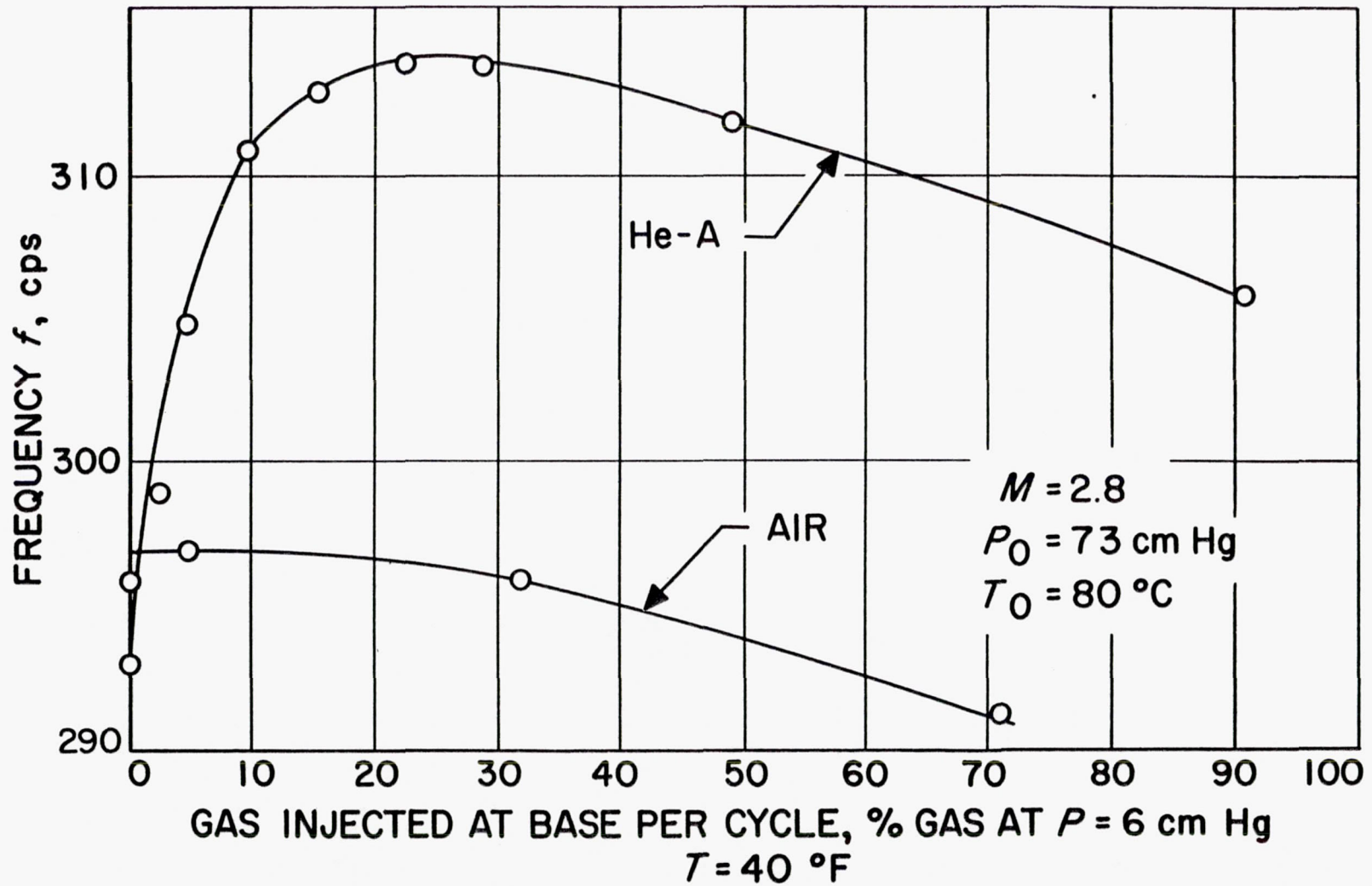


Fig. 11. Effect of adding He-A or air on resonant frequency

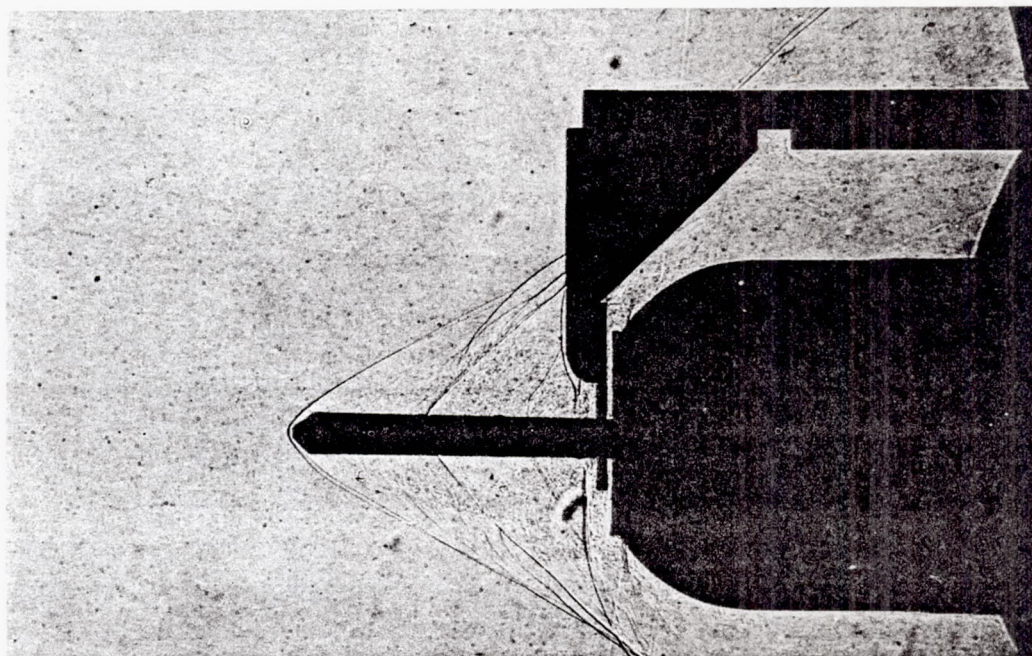


Fig. 12a. Spark shadow with disc gate in front of tube

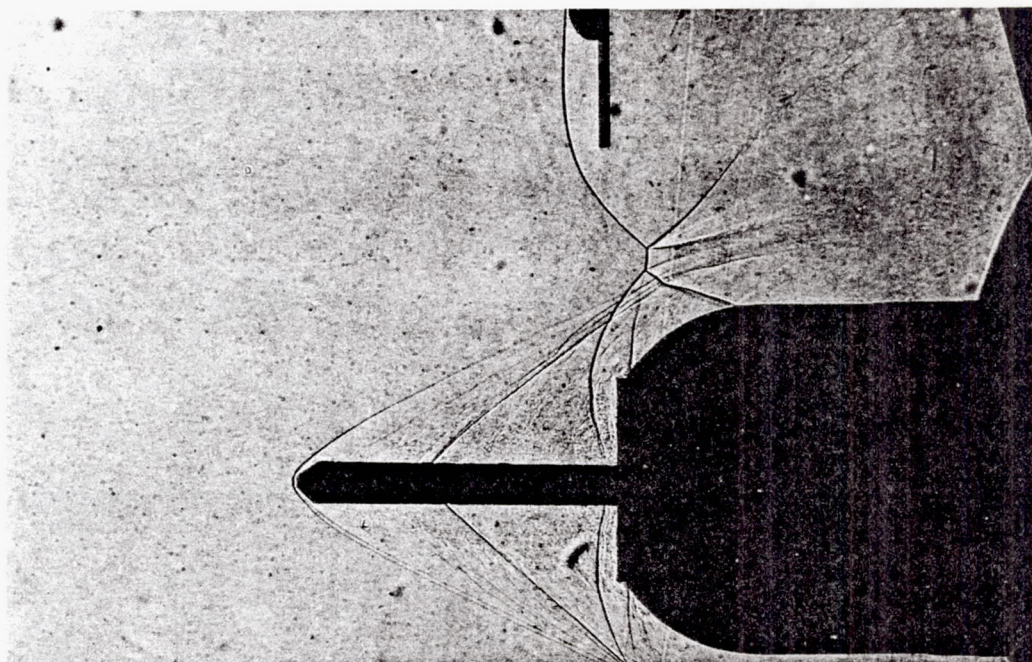


Fig. 12b. Spark shadow with disc gate removed

NOT REPRODUCIBLE

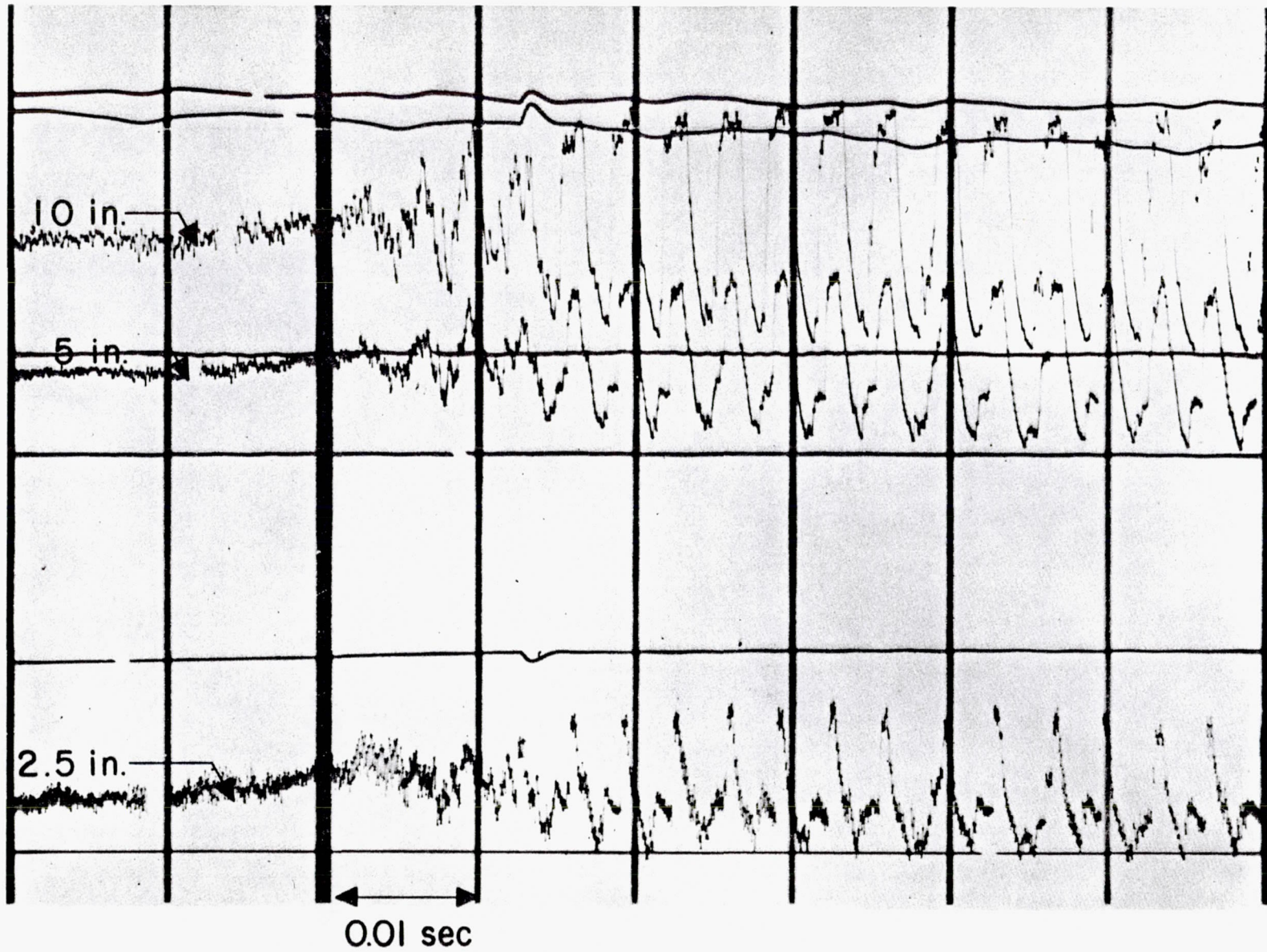


Fig. 13. Oscillograph record of pressures in the tube while the disc gate is being removed

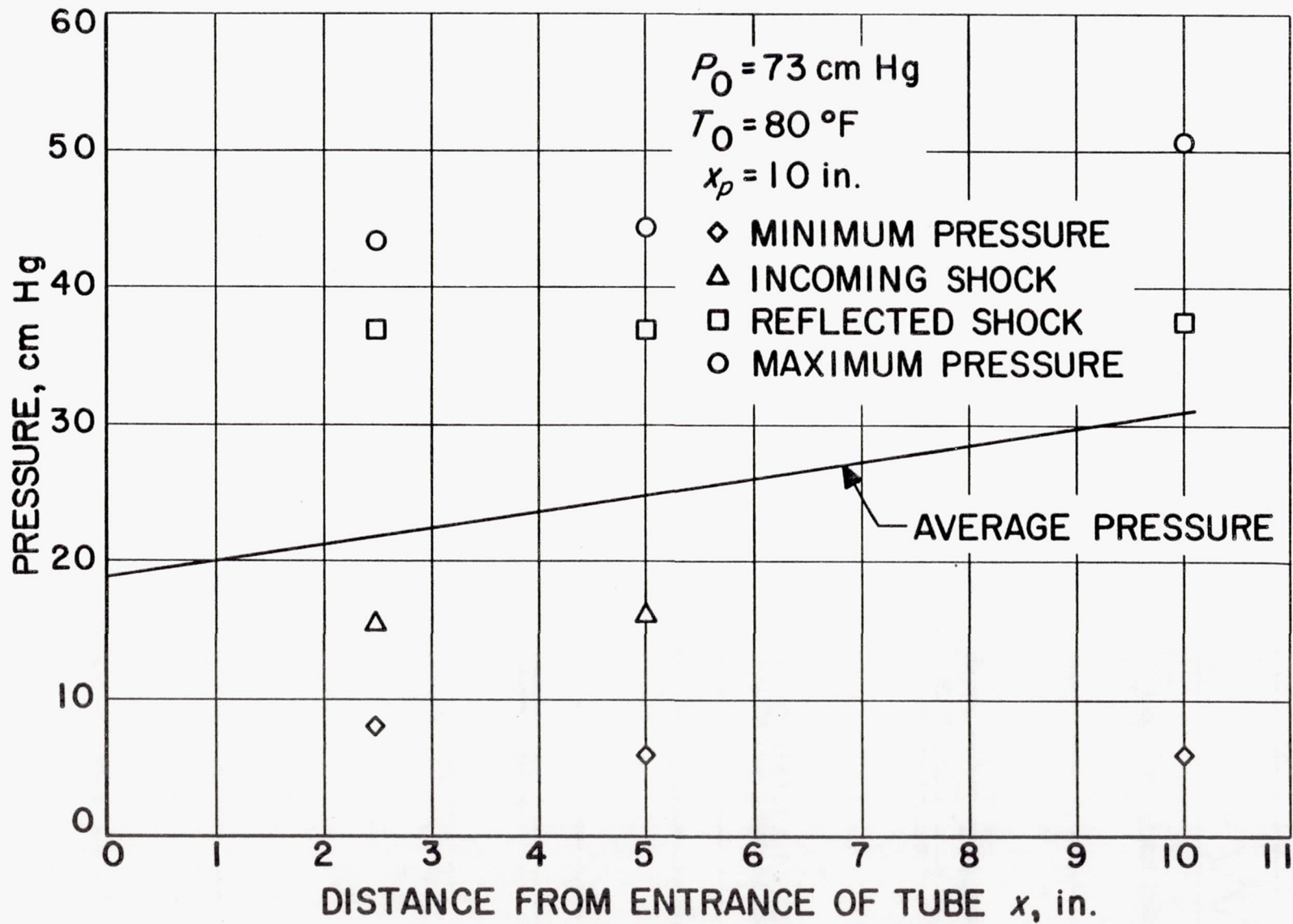


Fig. 14. Pressures determined from oscillograph record

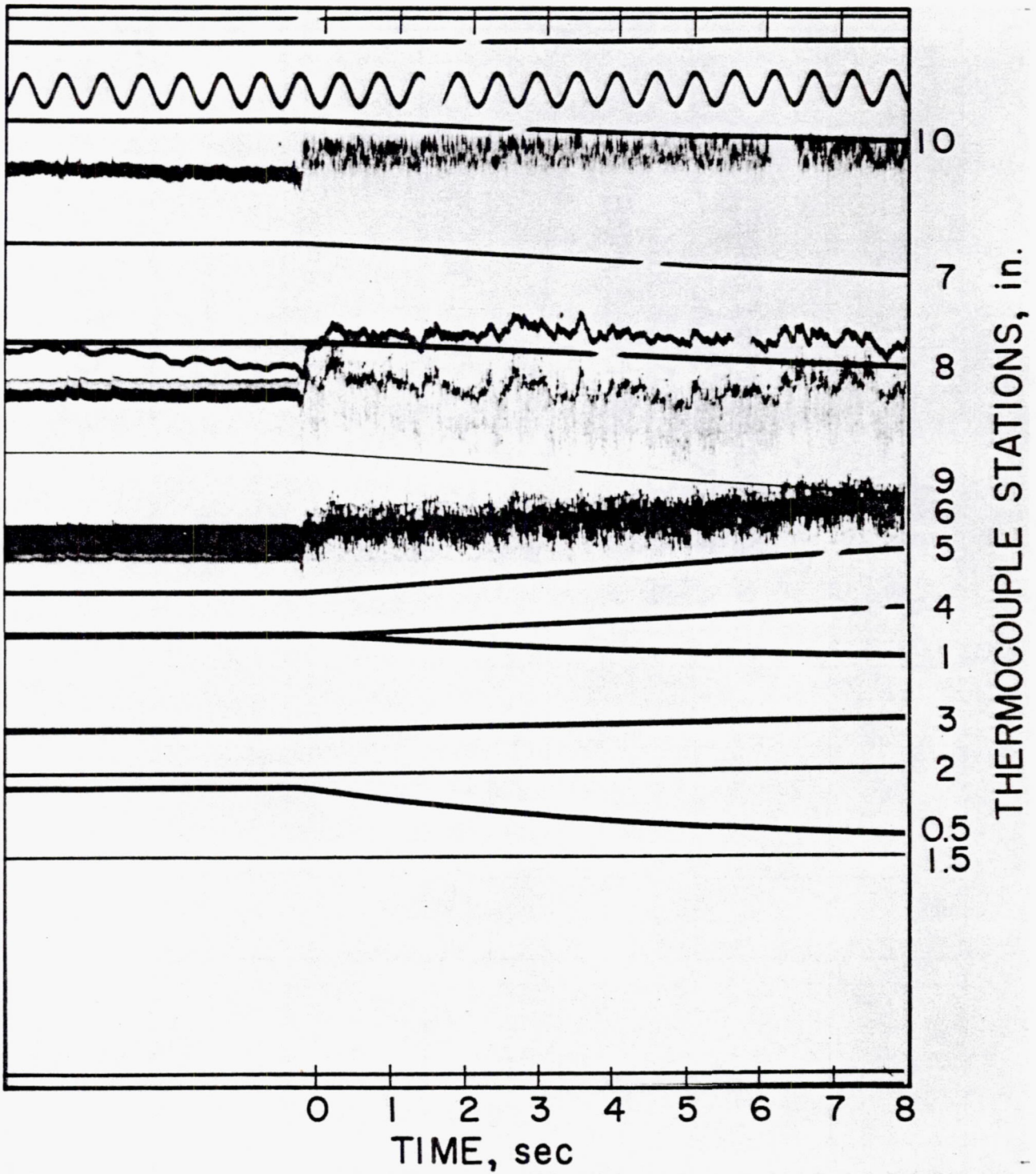


Fig. 15. Oscillograph record of thermocouple output while disc gate is being removed

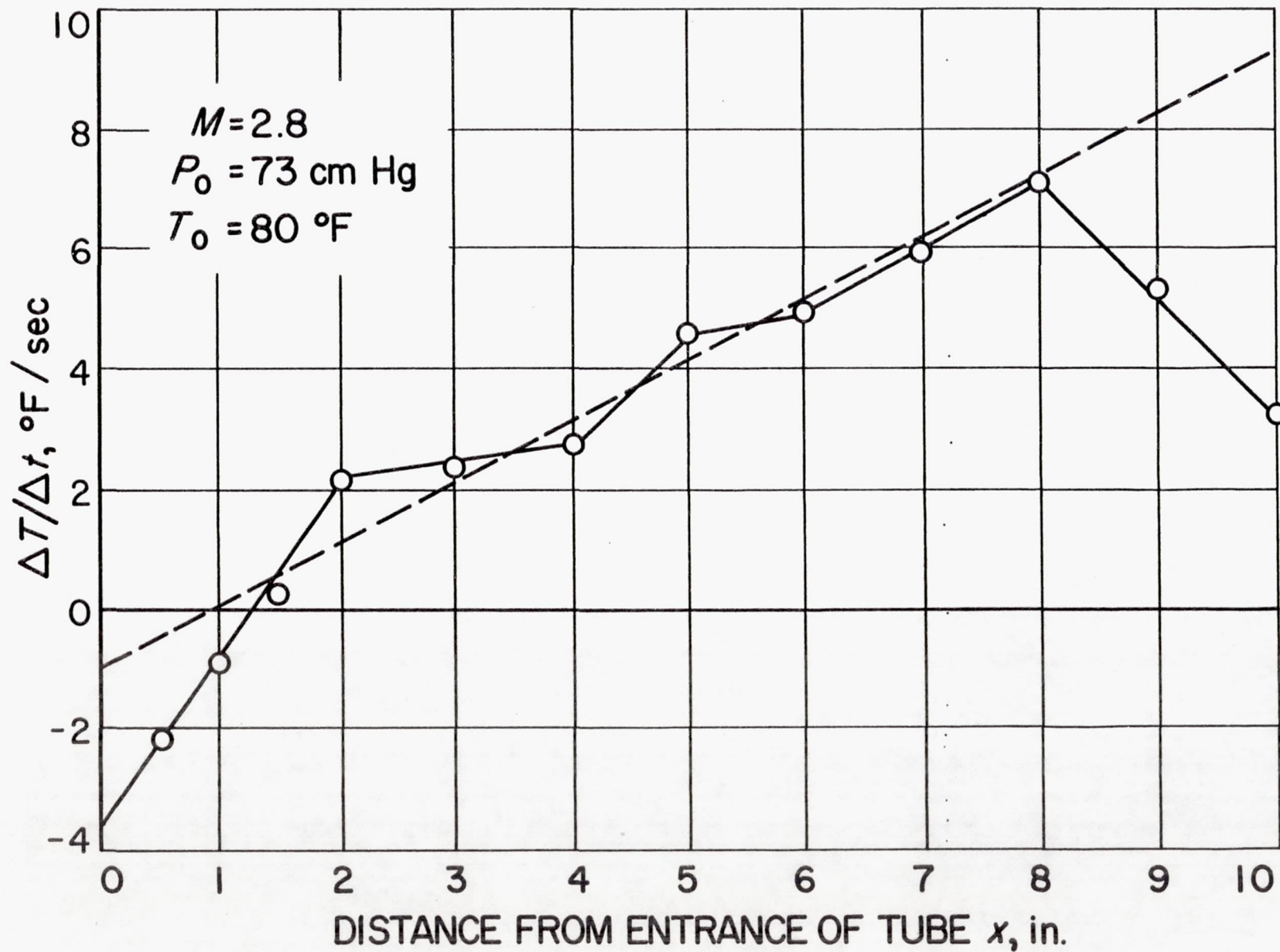


Fig. 16. Time rate of change of temperature at first instant after disc gate has been removed

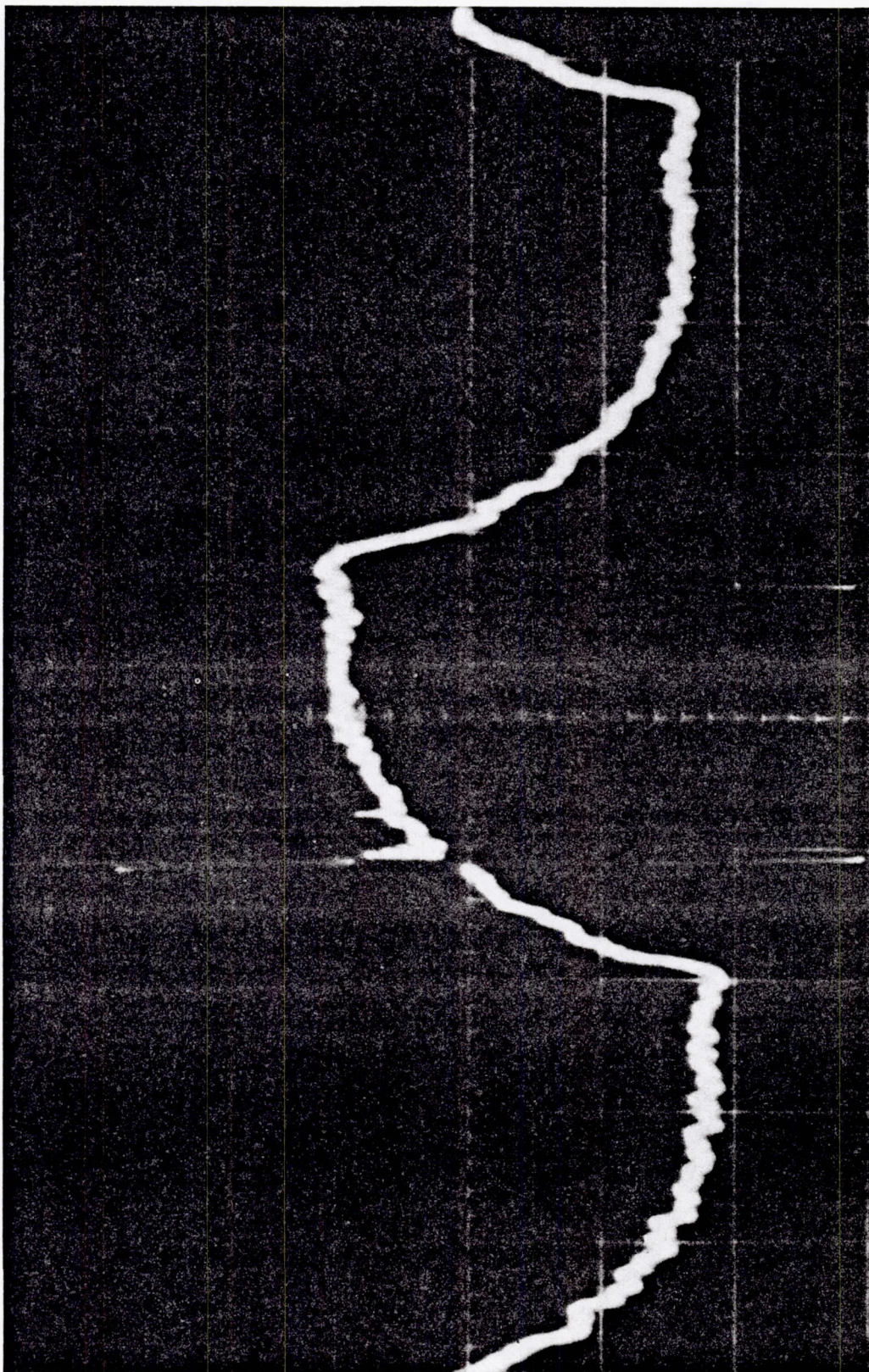


Fig. 17. Pressure at base of glass model without trip

NOT REPRODUCIBLE

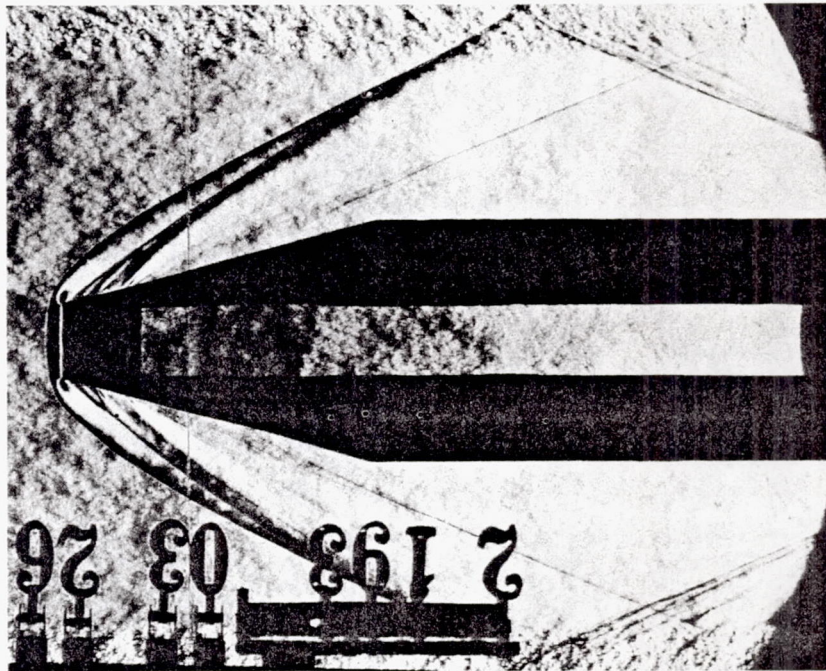


Fig. 18a. Spark schlieren photograph of glass-sided tube without trip, filling part of cycle

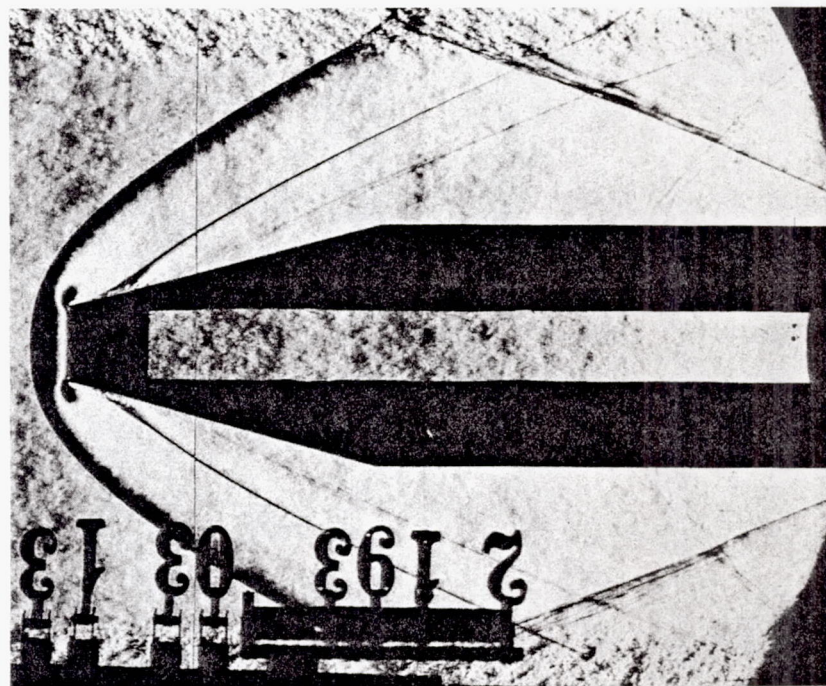


Fig. 18b. Spark schlieren photograph of glass-sided tube without trip, spilling part of cycle

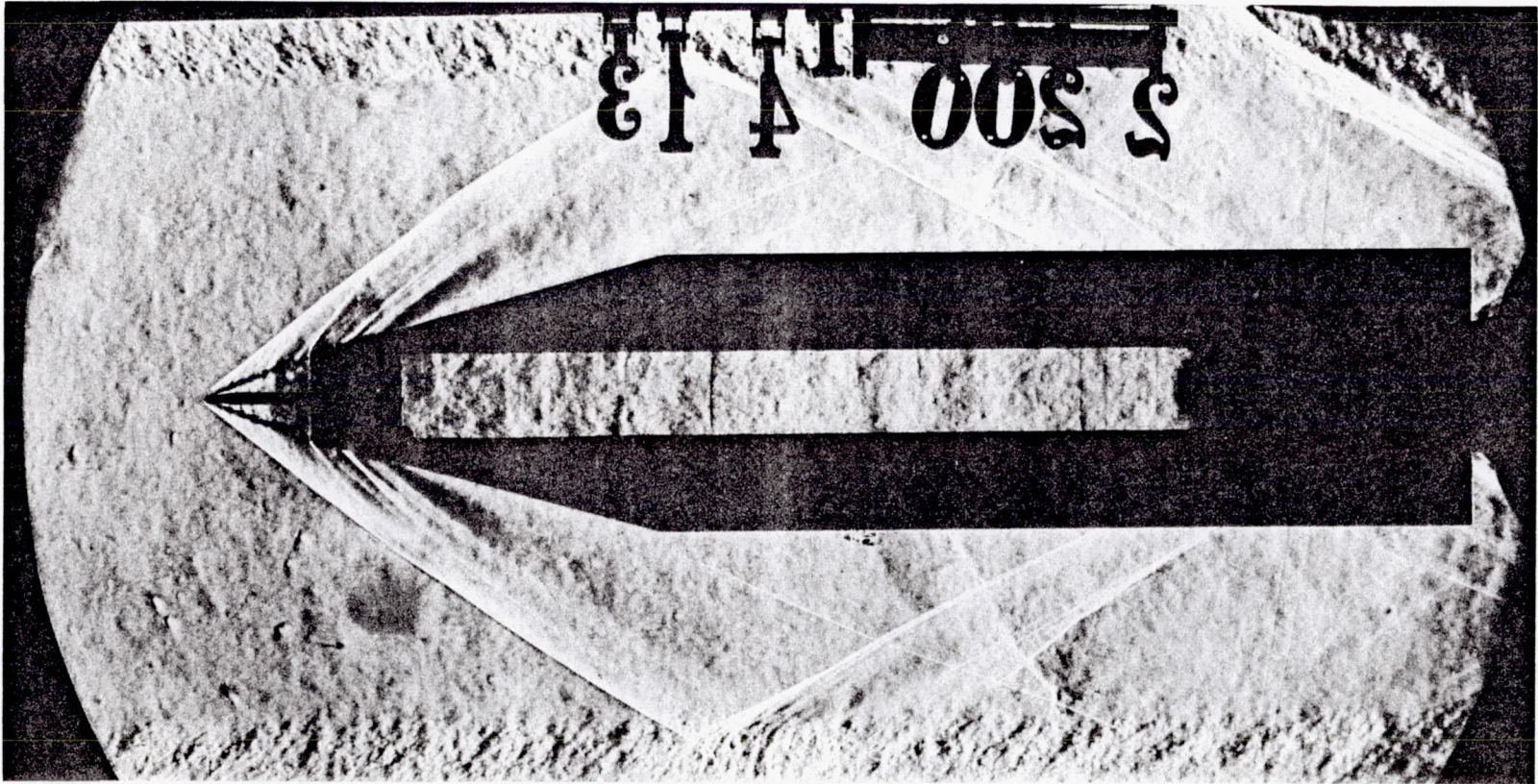


Fig. 19. Spark schlieren photograph of glass-sided model with trip

NOT REPRODUCIBLE

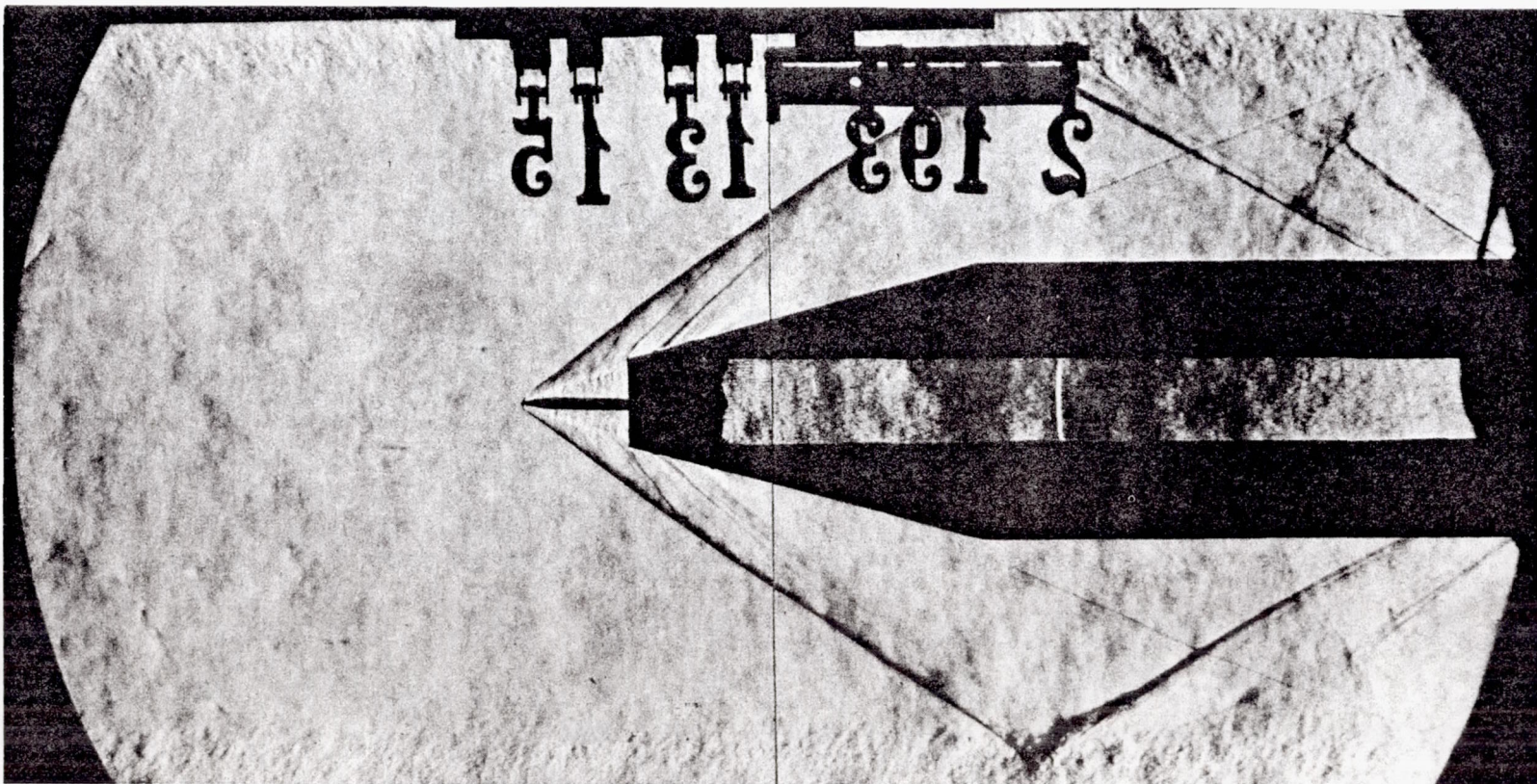


Fig. 20. Spark schlieren photograph of glass-sided model with trip and knife-edge rotated 180 deg

NOT REPRODUCIBLE

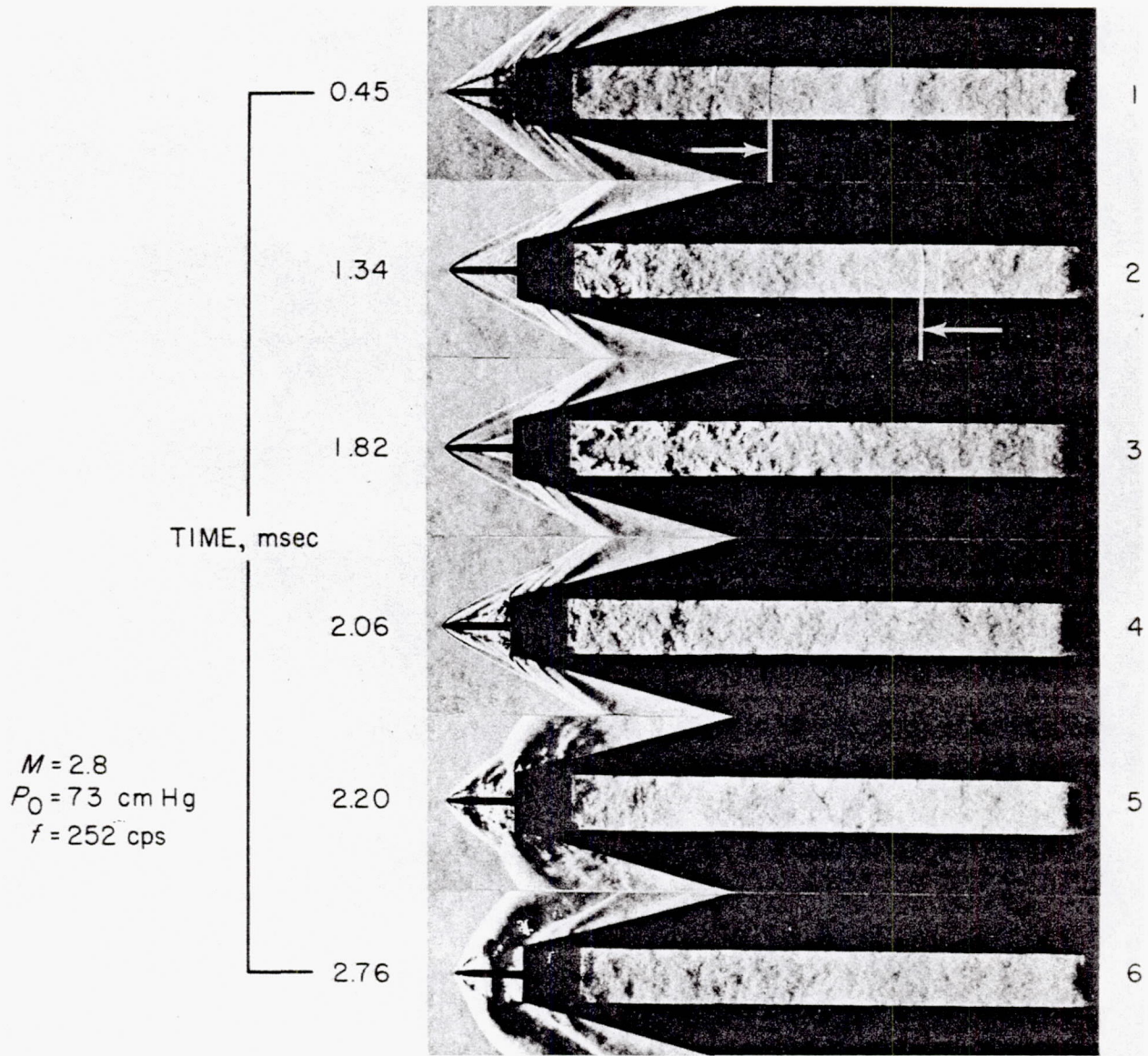


Fig. 21. Series of spark schlieren photographs of glass-sided model

NOT REPRODUCIBLE

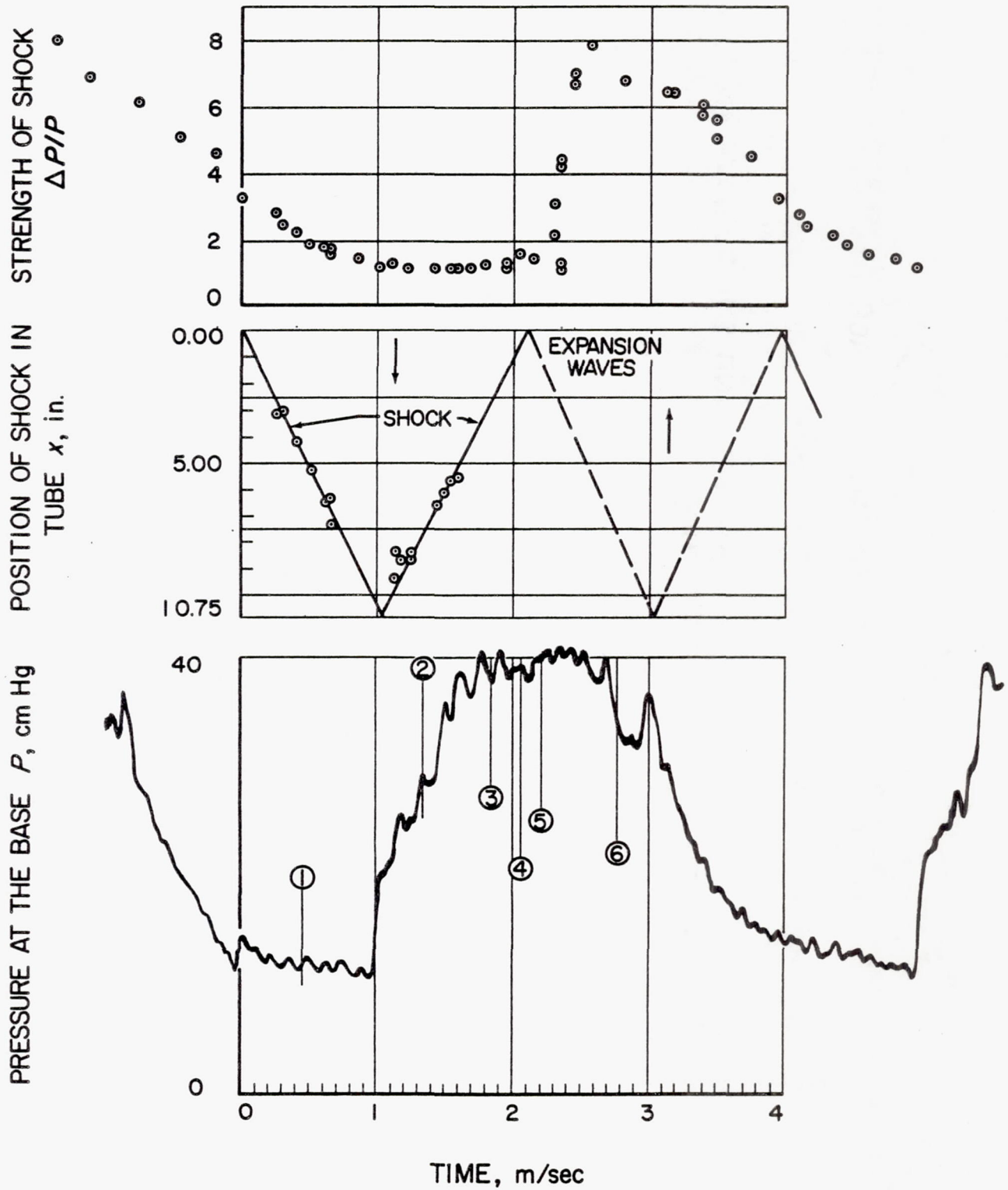


Fig. 22. Pressure at the base, position of shock wave intake, and strength of shock wave in front of the glass-sided tube

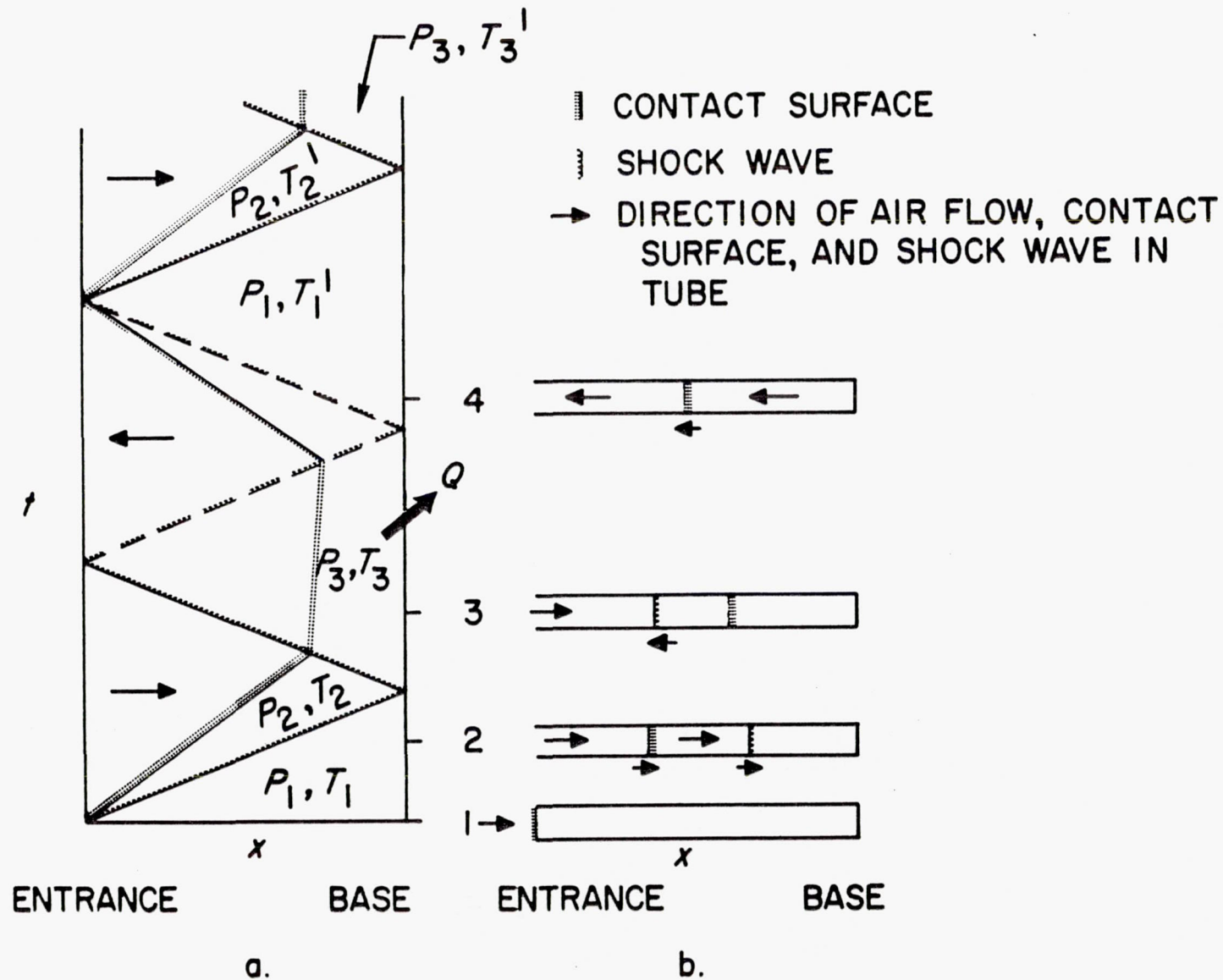


Fig. 23. Idealized resonance cycle

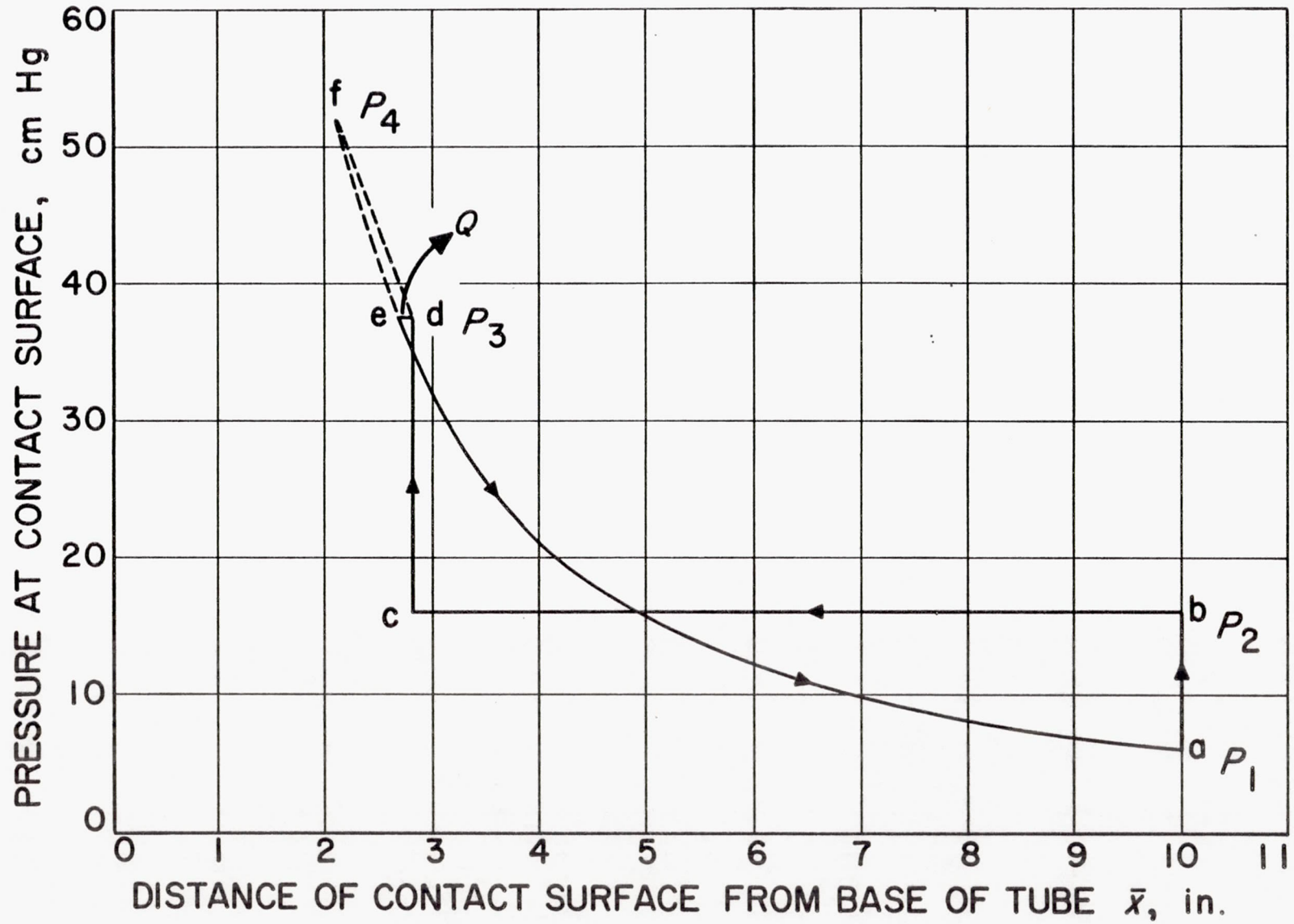


Fig. 24. Work at contact surface in resonance cycle, $P - \bar{x}$ diagram